FINAL REPORT

FIRETEC and WFDS Modeling of Fire Behavior and Smoke in Support of FASMEE

JFSP PROJECT ID: 16-4-05-1

JUNE 2017

William Mell (PI), Pacific Wildland Fire Sciences Laboratory, Pacific Northwest Research Laboratory, 400 N. 34th St., Suite 201, Seattle, WA 98103. Email: wemell@fs.fed.us.

Rod Linn (Co-PI), Earth and Atmospheric Sciences Division, Los Alamos National Laboratory, Los Alamos, NM 86001

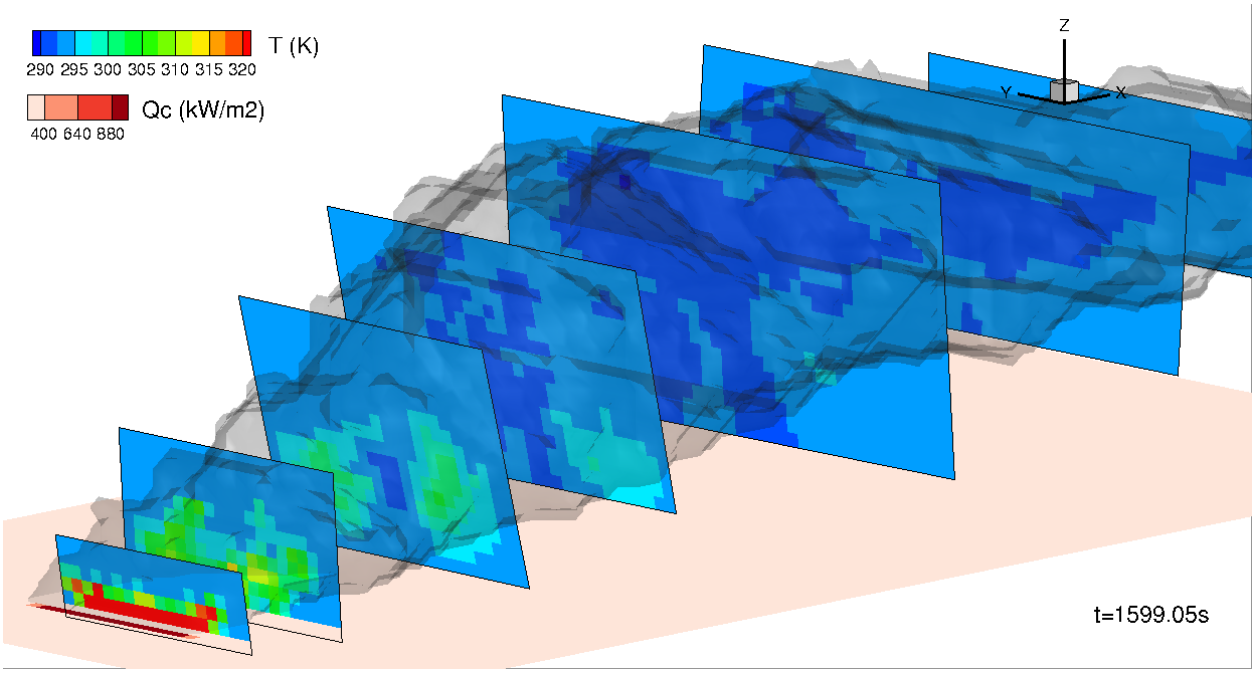

Table of Contents

List of Figures i
Abbreviations/Acronyms ii
Keywords ii
Acknowledgements ii
Abstract 1

1. Objectives 1

2. Background 2

3. Materials and Methods 3

4. Results and Discussion 3
   4.1. Lessons Learned from Relatively Small Burn Plots 3
   4.2. Lessons Learned from a Large Burn Plot in RxCADRE 4
   4.3. The Burner Method 7
   4.4. The use of Overhead Imagery for Support of the Burner Method 10
   4.5. Demonstration of the Burner Method for a Spreading Fire 14
   4.6. Smoke Plume Simulations – Idealized Case using a Fixed Line-Fire Burner 16
   4.7. Simulations of Fire on an Isolated Hill 20
   4.8. Field Measurement Needs 26
   4.9. Integrated Data Management Needs 27

5. Conclusions 28

Literature Cited 30

Appendix A: Contact Information for Key Project Personnel 32

Appendix B: List of Completed and Planned Publications and Science Delivery Products 34
   Conference Proceedings 34
   Conference Abstracts 34
   Posters 34

List of Figures

Figure 1: IR based fireline and fuel distribution from the (a) S3 and (b) Camp Swift burns. 4
Figure 2: Image of prescribed burn experiment 703C. 6
Figure 3: Example of connecting smoke plume models of different scales. 8
Figure 4: Fire front arrival time directly from imagery of prescribed burn 703C. 12
Figure 5: Fire front arrival time in prescribed burn 703C derived from interpolation. 13
Figure 6: Map of derived ROS for prescribed burn 703C. 13
Figure 7: Time histories of the total HRR of a spreading fire using WFDS-LS or burners. 15
Figure 8: Fireline HRRPUA (left) and plume (right) from WFDS-LS and burner simulations... 16
Figure 9: Simulated smoke plumes from a line fire (u_o= 5 m/s, LR = 0 C/km)..... 18
Figure 10: Simulated smoke plumes from a line fire (u_o= 1 m/s, LR = -6 C/km). 19
Figure 11: Plume centerline location for the u_o= 5 m/s, LR = 0 C/km, case. 19
Figure 12: Plume centerline location for the u_o= 1 m/s, LR = 0 C/km, case. 20

Figure 13: Fuel map for FIRETEC simulation of hypothetical ring fire on knob at Fishlake..... 21
Figure 14: U (west to east) component of the winds at 1.5 m above the ground. 24
Figure 15: V (south to north) component of the winds at 1.5 m above the ground. 24
Figure 16: Visualization of a FIRETEC simulation of Fishlake site. 25

Abbreviations/Acronyms

CFD	Computational Fluid Dynamics
FASMEE	Fire and Smoke Model Evaluation Experiment
FRP	Fire radiative power
GSAT	Geospatial science and technology
HRR	Heat release rate (kW)
HRRPUA	Heat release rate per unit area (kW m^{-2})
LiDAR	Light Detection and Ranging
LR	Lapse rate (C/km)
MIR	Middle infrared
NED	National Elevation Dataset
NIR	Near infrared
ROS	Rate of spread
RxCADRE	Fire Combustion and Atmospheric Dynamics Research Experiment
SWIR	Shortwave infrared
TIR	Thermal infrared
UAS	Unmanned aerial systems
WASP	Wildfire Airborne Sensor Program
WFDS-PB	Wildland-urban interface Fire Dynamics Simulator – Physics Based
WDFS-LS	Wildland-urban interface Fire Dynamics Simulator – Level Set based

Keywords

DaySmoke, FIRETEC, MesoNH, WFDS, WRF

Acknowledgements

Discussions with Derek McNamara (Geospatial Measurement Solutions, Oregon, USA) over a range of topics are greatly appreciate as are the RxCadre and Camp Swift data integration's he provided. We would like to thank the following for providing their results for the simulation of a smoke plume from a stationary line fire burner: Adam Kochanski (University of Utah, Atmospheric Sciences, Utah, USA) the WRF-SFIRE model and Yongaiang Liu (U.S. Forest Service Southern Research Station, Georgia, USA) the DaySmoke model. We also thank Jean-Baptiste Filippi (University of Corsica, France) for his assistance with running the MesoNH-ForeFire simulations of smoke plumes from a stationary line fire burner and Susan Prichard and Benjamin Bright for contributing to the development of fuels and topography inputs for FIRETEC simulations

Abstract

The objective of FASMEE is to obtain measurements that can be used to evaluate and advance operational smoke models. Among the focus areas listed in the FON task statements are the modeling of fire growth, fire behavior, and plume development. In current operational models, the physical processes driving fire growth, fire behavior, and plume development are not explicitly modeled. These processes are, however, explicitly modeled in physics-based fire behavior models that use the methods of computational fluid dynamics (CFD). Thus, these physics-based fire behavior models, if suitably validated, could be used to help advance operational smoke models. Validation of physics-based fire behavior models, however, requires a wide range of environmental and fire behavior information. Obtaining sufficient information for comprehensive validation of physics-based models through field measurements is challenging – significantly more so than validation of empirically based fire spread models. These measurement challenges are essentially insurmountable for large burn plots with fires that are significantly influenced by local changes in vegetation and wind. Complex ignition procedures increase the measurement challenges. Most FASMEE burn sites are large in area, will use complex "ping pong" ball ignition procedures, and are expected to be of low to moderate fire intensity, typical of prescribed burns. As such, these fires are likely to be influenced by local variations in wind and/or vegetation. In summary, the large area, low to moderate fire intensity, prescribed burns of FASMEE are not suitable for validation of the fire behavior predictions by present-day CFD physics-based models.

Any physics-based fire behavior model using CFD methods can also predict smoke plume rise, due to a heat source that represents a wildland fire, and subsequent downwind transport of smoke. Here, we call this heat source a burner. The burner approach has been used successfully for modeling smoke plumes from burning oil spills. As part of this project, a simple burner demonstration using five different smoke models was conducted. Thus, a range of CFD-based fire behavior and smoke models can be applied to the smoke rise and transport problem by representing the fire as a burner. This facilitates model comparison and model improvement, and provides guidance to measurements needs. Implementing the burner method requires the time history of the heat release rate per unit area (HRRPUA) across the burn plot. This can only be obtained through overhead remote sensing that is suitably calibrated by ground instrumentation. Also, the quantities needed to obtain the HRRPUA can be used to support coarse testing of fire behavior models.

Finally, there is a critical need for the use of geospatial science and technology practices to ensure that the measurements are properly co-located in space and time, quality assured, well-documented, and made publicly available in an effective manner.

1. Objectives

In our original proposal, we planned to provide guidance on field measurements that would support the validation of physics-based fire behavior models. However, we were concerned that unless the experiments were designed with vegetation, wind, and terrain conditions that resulted in a sufficiently "well-behaved" fire, the environmental and fire measurements required to capture the fire behavior would be prohibitively difficult. This is discussed further in Section 2.

It became clear during FASMEE Phase I discussions that 1) the highest priority for FASMEE data collection was to provide data sets to support the development and validation of smoke plume models, 2) both the expected dynamic fire behavior and the complex ignition procedure, planned for most of the FASMEE burns, would not be amenable to a measurement effort that could produce validation datasets needed for physics-based fire models. The exception to this is maybe burns a southwest site with a single fireline spreading upslope and a large fireline depth.

For the above reasons, the focus of this project shifted to determining what measurements would best support smoke plume model validation, especially from the point of view of what fire behavior measurements would be needed to inform smoke models of the heat source due to the fire. This led to the development of what is called the burner method and an effort to identify the field measurements required to support its implementation. The burner method is the most direct approach to providing heat source information to a range of models capable of simulating plume rise and subsequent smoke transport. In addition, we assessed the use of overhead imagery to support the burner, and compared smoke plume simulations from five different smoke plume models, each uses a simple implementation of the burner method, in order to help identify measurement needs and assess the state of these models. We also conducted exploratory simulations with the burner method on level terrain and a spot (ping pong ball) ignition in complex terrain.

2. Background

Both FIRETEC (Linn, 1997; Linn and Cunningham, 2005; Linn et al., 2005) and WFDS-PB (Mell et al., 2007; Mell et al., 2009) are physics-based wildland fire models that use the methods of computational fluid dynamics (CFD) to simulate the component physical processes that drive fire behavior. Some examples of the physical processes of interest are the drying, pyrolysis, and char oxidation of the vegetation; gas-phase heat transfer (convective and radiative) and combustion; and smoke generation and transport. Examples of fire behavior characteristics are the overall consumption of the vegetation, spread rates and fire depth along the fire perimeter, plume rise, and smoke profiles. The WFDS model can also be implemented in a manner that uses empirical formulas for the spread rate along the fire perimeter and propagates the perimeter using a level set method. This implementation is called WFDS-LS (Bova et al., 2016; note that changes to WFDS-LS have been made since Bova et al. that model, a simple way, fire-atmosphere interactions).

The validation of physics-based models, is supported by measurements of both the component physical processes and the resulting fire behavior. Validation of models for the component processes requires data sets from repeatable experiments in which many of the environmental conditions are well characterized, thereby allowing a focus on one or a few physical processes of interest. This is best accomplished in the controlled and repeatable conditions of laboratory or (potentially) small-scale field burns.

Field experiments lack the repeatability of laboratory experiments and their larger scale makes it very challenging to conduct spatially detailed measurements of a process of interest and, thus, are best suited for measurements supporting validation of fire behavior predictions. However, even when measurements are aimed at capturing fire behavior they face significant challenges.

This is mostly centered on the fact that it is unknown a-priori how resolved in space and time the environmental and fire behavior measurements should be in order to create a useful validation dataset. In fact, the spatial and temporal resolution requirements depend on the environmental conditions (e.g., variability in the wind and vegetation) and the fire behavior (e.g., variability in ROS, fireline depth, and fireline continuity).

When designing a field experiment for validation of physics-based wildland fire behavior models, great care must be taken to ensure that the fire behavior is not significantly influenced by local changes in the wind and vegetation (i.e., gusts or fuel heterogeneity) or the ignition procedure that are not, or cannot, be adequately measured. Thus, it is very advantageous to choose vegetation and wind conditions that result in expected, although potentially dynamic, fire behavior. This allows for the design and implementation of a field experiment that will sufficiently capture the fire behavior to provide a useful validation dataset.

The key point here is that the variations in vegetation and wind (and the ignition procedure) are *sufficiently measured*, supporting a clear connection to the observed fire behavior. This is especially challenging for fires that are expected to be sensitive to local changes in vegetation, terrain, and wind. Thus, lower intensity, slower spreading, prescribed fires spreading in light ambient winds through surface fuels that are heterogeneous, either in type and or in spatial distribution, are likely to be especially challenging to adequately measure. Also, ignition procedures that are not well controlled or well characterized cannot be reproduced by the fire model, leading to model prediction errors. Furthermore, some characterization of both measurement and experimental error is needed to support a well-founded validation study.

3. Materials and Methods

This is a strictly modeling and retrospective study. The models used are described below.

4. Results and Discussion

As discussed in Section 2, field experiments that seek to create validation datasets for physics-based fire behavior models need to sufficiently measure the environmental conditions (i.e., characteristics of the vegetation and local winds) that are relevant to the observed fire behavior. In the next two sections, we assess some past experiments with this criteria in mind.

4.1. Lessons Learned from Relatively Small Burn Plots

We consider three field experiments. All three experiments were designed with the intent of supporting the testing and development of physics-based fire behavior models. Ignition occurred via drip torches with the objective of obtaining a well characterized and continuous initial fireline. Two experiments had surface fuels only: the S5 (100 m x 200 m) experiment of RxCADRE (Ottmar et al. 2016) and the Camp Swift experiment (100 m x 100 m) (McNamara 2015 a,b). The third experiment (~ 200 m x 200 m) occurred in the New Jersey Pine Barrens which had an overstory dominated by pitch pine, an understory of shrubs, and litter dominated by needles (Mueller et al. 2017). Due to space constraints, these experiments cannot be described in detail here. Only the aspects and outcomes of the experiments that are relevant to the present discussion are considered.

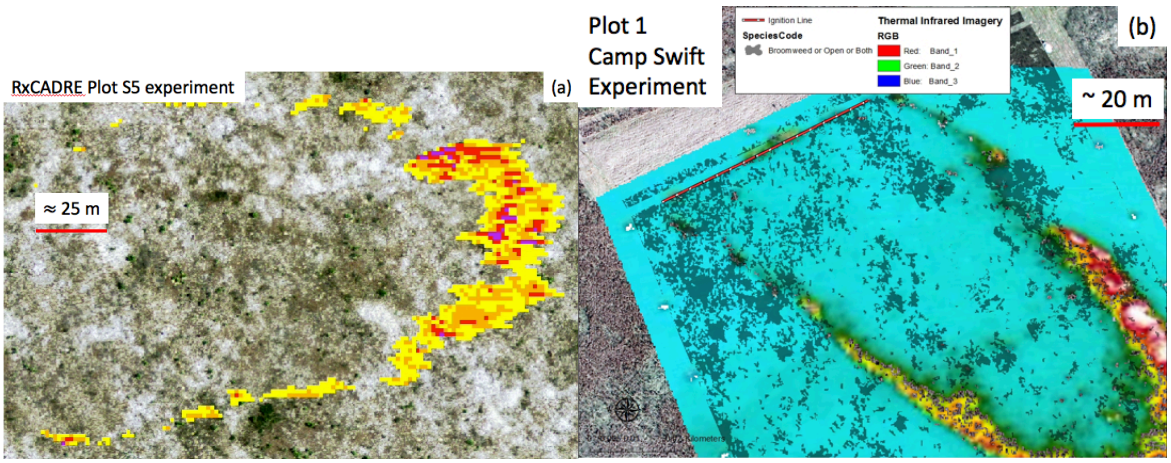

Figure 1: IR based fireline and fuel distribution from the (a) S5 [see O'Brien et al. 2106]and (b) Camp Swift burns.
[from D. McNamara].

Figure 1 shows GIS layers of the firelines, based on IR measurements, and the vegetation distribution. In each case the head fire is continuous, but the flank fires are not most likely due to inhomogeneity in the vegetation. In Figure 1(a) the flank fire breaks apart due to the absence of vegetation (denoted by white areas), in Figure 1(b) this occurs due to the presence of less flammable vegetation (denoted by dark shading). A validation dataset would require the characteristics and distribution of vegetation at spatial scales relevant to the behavior of the flank fire, which for these fire is approximately 1 m. It's worth noting that challenges have been encountered distinguishing grass and bare soil/sand using LiDAR (Rowell et al. 2013) and vegetation samples taken outside the plot may not reproduce conditions in the plot (Rowell et al. 2017). The importance of adequately measuring the spatial distribution of surface and litter fuels in order understand unsteady fire behavior in the Pine Barren experiments is also noted in Mueller et al. (2017).

Wind can also play an important role in causing unsteady fire behavior. The burn plots in Figure 1 had anemometers along their perimeter at approximately 20 m spacing. Unsteady behavior in the western flank fire of Figure 1(b) at later times (changes in the vegetation did not appear to contribute to this) was correlated with an observed wind shift in the anemometers along the western plot perimeter. However, this wind shift was not observed in the other anemometers along the perimeter. This implies that changes in the wind, relevant to fire behavior, can occur over distances less than approximately 50 m.

In conclusion, creating a validation dataset for physics-based fire behavior models is very demanding measurement task for fires that are significantly influenced by variation in vegetation and local winds. The examples above imply a sampling resolution for vegetation (1 m or less) and wind (50 m or less). For sufficiently small burn plots, this may be possible. For large area plots, such as proposed for FASMEE, this is prohibitive.

4.2. Lessons Learned from a Large Burn Plot in RxCADRE

In 2011, the prescribed burn experiment, 703C was conducted at Eglin Air Force Base, Florida (Ottmar et al. 2016)). The smoke plume from this fire was the subject of a simulation study of

Achtemeier et al. (2012). Figure 2 is a georectified image showing the location of the fire, as detected from an overhead long-wave infrared camera mounted on an airplane (Wildfire Airborne Sensor Program (WASP)) flying in an east-west loop (Hudak et al., 2016(a)). The field of view of the camera did not cover the entire east-west extent of the burn plot (which is approximately 3 km x 2 km); it did cover the north-south extent. For this reason, the IR image in Figure 2 is obtained from a number of consecutive images taken during the fly-over. Canopy height derived from Light Detection and Ranging (LiDAR) data is shown with green shading and the terrain variation from LiDAR with gray shading. The ambient wind was roughly south to north with a speed of 1.4 m/s at 10 m above ground. The fire was ignited by dropping "ping pong ball" chemical ignition devices from a helicopter which was flying back and forth across the plot in the east – west direction. Upon reaching the eastern or western plot edge, the helicopter flew south for approximately 100 m before starting the next east – west transit. Thus, ignition started at the downwind edge of the plot (top of Figure 2) and ignition "lines" were separated by approximately 100 m. The ping pong balls were dropped approximately every 0.5 s resulting in a spacing of about 12 m on the ground.

The outcome of the ignition procedure used in experiment 703C, and seen in Figure 2, is typical of prescribed burn procedures (for large area burn plots) and is proposed for most of the FASMEE burns. This figure was created based on measurements from a number of experimental efforts: Hudak et al. 2015 for radiometer locations; Hudak 2014 for ground cover fractions; Hudak et al. 2014(a) for clip plot locations; Hudak et al. 2014(b) for burn blocks; Hudak et al. 2016(b) for long wave IR; Hudak et al. 2016(c) LiDAR intensity

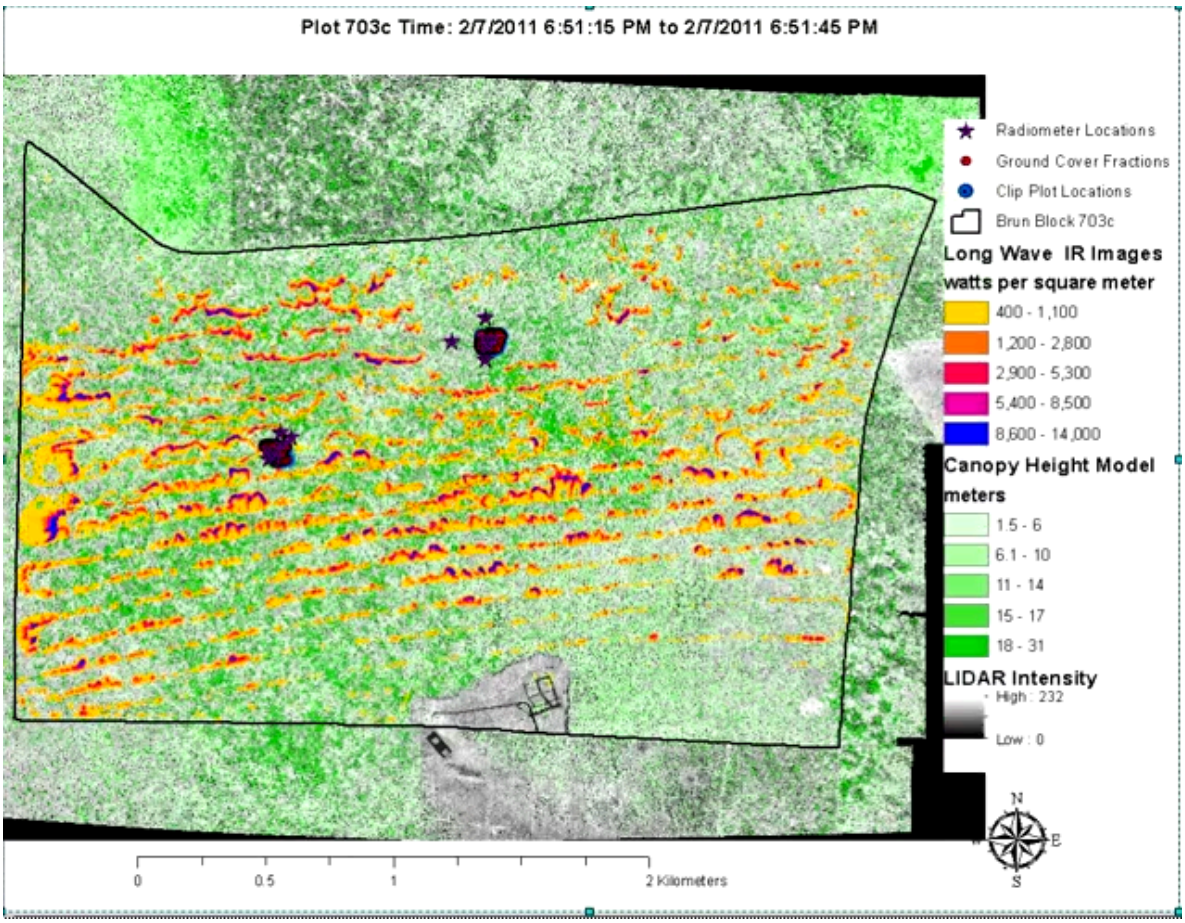

Figure 2: Image of prescribed burn experiment 703C.
This image is a GIS overlay of pre-fire and during fire conditions using frames from the overhead IR camera over a 30 s time interval. (From D. McNamara using a number of datasets available on the USDA Archive (2017)).

The fire behavior in Figure 2 can clearly be seen to vary significantly along an east – west ignition path. For example, on some ignition paths the fire is larger at later times, contrary to what would happen if the local winds, vegetation, and ignition outcomes were uniform. AS discussed in Section 4.1, determining the source of the observed differences along an ignition path (i.e., the combined differences in ground and surface vegetation, local winds, or ignition outcomes when the ping pong ball hit the ground) would be a tremendous, if not impossible, measurement effort (it did not occur for the 703C burns). For this reason, it will not be possible to conduct field measurements, for most of the FASMEE burns, that would result in fire behavior validation datasets for physics-based fire models. The exceptions to this may be the isolated knob burns and the planned upslope, single line, stand replacing fire because the expected large fireline depth could result in fire behavior that is insensitive to changes in the surface and ground fuels – but this is not conclusive. Simulation of a knob burn is discussed below in Section 4.7.

In addition to the measurement challenges discussed above, FASMEE's candidate burn plots are, in general, too large to be simulated by current physics-based fire behavior models that explicitly model combustion (e.g., FIRETEC, WFDS-PB). This becomes more the case for fires with smaller fireline depth. From a purely numerical point of view, these models need to have

sufficiently fine computational grids to adequately resolve the fireline depth and the combustion processes that drive the formation and rise of the smoke plume.

For the sake of illustration, if we assume the fireline depth needs to be covered by 3 grid cells and we have 500 cpus, then (based on the memory and speed of operation characteristics of the WFDS-PB model) resolving a meter deep fireline would restrict the computational domain size to approximately 240 m on a side (i.e., a cubed shaped domain). This domain size scales linearly with the fireline depth: the maximum computational domain for a 10 m deep fireline is approximately 2600 m on a side if 500 cpus are available.

Based on the analysis in this and the previous section, and since the primary focus of FASMEE is measurements to support improvements in plume rise and smoke transport modeling, effort here was put into identifying the gross fire behavior measurements that are most important from the point of view of supporting smoke plume simulations. This led to the identification and formulation of the burner method which is described in the next section. The advantage of the burner method, for modeling, is that the fire behavior itself does not need to be explicitly modeled.

4.3. The Burner Method

The primary measurement goal of FASMEE is the creation of an observational database that supports the implementation and evaluation of models that simulate the rise and subsequent transport of smoke from prescribed fires in wildland fuels. This requires that the measurements meet the needs of a range of "smoke" models. These models differ in their input needs, scale of operation, and computational cost. Here, we put the models into two groups:

A. Models that simulate the plume rise explicitly (e.g., DaySmoke-RabbitRules [Achtemeier et al., 2012], FIRETEC [Linn 1997; Linn and Cunningham 2005; Linn et al. 2005], MesoNH-ForeFire [Filippi et al. 2009], WFDS [Mell et al. 2007; Mell et al. 2009], WRF-SFIRE [Mandel et al. 2011; Mandel et al. 2014). These explicitly capture, to varying physical fidelity, fire behavior (e.g., the fireline and its spread).
B. Models that operate over large scales (~100 km) and do not simulate the plume rise explicitly (e.g., BlueSky [Larkin et al. 2010], CMAQ [CMAQ 2017]; VSMOKE [Lavdas 1996]). These do not capture the fireline, instead the fire is an area source of heat and mass.

The focus here is on models in group (A) because the expectation is that the data collected during FASMEE will support improvements to the explicit modeling of plume rise which, in turn, will result in improvements in the simplified accounting for plume rise in the group (B) models. A similar connection between models operating at different scales has been implemented before in the context of modeling smoke rise and transport from burning oil spills, see Figure 3 (McGrattan et al. 1997).

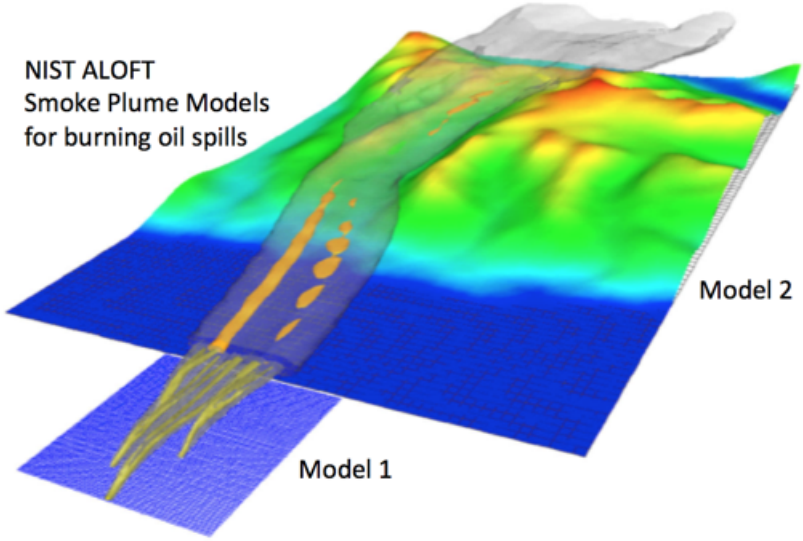

Figure 3: Example of connecting smoke plume models of different scales.
Model 1 and Model 2 are analogous to the models in group A and B, respectively, which were discussed above. Model 1 (operates over kilometers) and explicitly captures plume rise and "hands off" the smoke characteristics to Model 2 (operates over 10s of kilometers) for the simulation of longer range smoke transport and dispersion.

In the normal operation of the group (A) models, the generation of the smoke plume is controlled by the fire behavior sub-model. Unfortunately, there is a scarcity of field experiments that produced datasets of fire behavior measurements suitable for physic fire model evaluation. The best field experiments, to-date, occurred in relatively homogeneous environmental scenarios. The Australian grassland experiments are an example. They had a uniform fuel, well-behaved wind, and a simple ignition procedure resulting in a well-defined, freely evolving fire line. The lack of comprehensive fire behavior model validation will result in uncharacterized errors in smoke plume modeling. Note this assumes that the computational challenges discussed in the previous section are not present or a simpler, computationally cheap, fire behavior model is used.

If the fireline depth is large enough and the fire sufficiently well behaved, the measurement and modeling challenges that have been discussed above may be manageable, but it is unlikely that this will be the case for most of the FASMEE burns. Thus, it will be advantageous to identify the measurements that will support first order smoke plume simulations by the models in group (A). The ALOFT model suite developed by NIST, and demonstrated in Figure 3 provides guidance. The plume rise portion of ALOFT does not explicitly model combustion. Instead, the estimated heat release rate per unit area of the pool fire (i.e., a burner) was prescribed based on measurements of mass loss rate.

The major benefit of the burner method for modeling is that it provides the group (A) models with sufficient information to model plume rise without having to model wildland fire behavior (e.g., fire spread). Instead, the time history and location of the heat and mass generated by the fire is prescribed based on the field measurements. Note, that the measurements required to

implement the burner method (which are listed below) would also support fire behavior model evaluation.

The burner method provides guidance and prioritizes the measurements. The key measurements are the minimum set that support the determination, at all locations of active flaming relevant to smoke plume formation, the time course of the heat generation by the fire. There may be areas of smoldering. These would need to distinguished from flaming, but implementation model in the smoke model would be the same, whether for flaming or smoldering. The following discussion is in the context of implementing the burner method for flaming portions of the landscape.

Measurements needed for implementation of Burner Method
In general, the burner method needs the following co-located in space and time measurements and information. These measurements and information are a minimum set and details will need to be worked out in Phase 2 of FASMEE.

1. Characterize the fuel consumption and the depth and residence time of the fire front at locations of sufficient heat generation to influence the formation and rise of the smoke plume. More specifically, key measurements will include:
    - Fuel consumption from pre-fire and post-fire fuel measurements to be used with the flame residence time to estimate the consumption rate and, therefore, heat release rate per unit area.
    - Qualitative airborne infrared and/or visible imagery at the highest spatial and temporal resolution possible to obtain the leading edge of the fire front location (e.g., fire arrival time).
    - Quantitative airborne infrared imagery to estimate local fire depth; 2D interpolation could be used to evaluate flame front depth for the whole plot.
    - Strategically placed ground-based measurements of the local evolution of fuel temperature (e.g., thermocouples strategically placed across the burn units in association with overhead imagery, quantitative fire radiation measurements on towers or some remote system) to estimate flame residence time and flame front depth. This latter would be compared with estimates from the quantitative airborne infrared imagery.
2. Pre-fire vegetation and terrain measurements are needed to help develop the strategy for locating the ground-based fire measurements to support the remote-sensing based determination of the depth, residence time, and heat release rate of the flame front across representative environmental conditions. Note, that the spatial distribution, loading, and type of ground litter is of predominate importance to fire behavior in most prescribed burns. This vegetation type is especially difficult to obtain from aerial remote sensing especially when a canopy is present.
3. Gather and document information from the FASMEE burn bosses and past experiments (e.g., RxCADRE. Peterson and Hardy 2016) on expected fire behavior (e.g., fire depth, spread rates, and the influence of vegetation types), ignition procedures, and measurement performance (when available) for each candidate site. This is critical for assessing the scope, location, and the resolution of both the ground and airborne based measurements.

Model simulations may help to characterize the minimum required spatial and temporal resolution of the overhead imagery and experimental design. But simulations would be best constructed with guidance from items 2 and 3 above so that they are based on environmental conditions and ignition procedures that are characteristic of the FASMEE experiments.

It is worth repeating that the burner approach will support a range of smoke plume rise models.

4.4. The use of Overhead Imagery for Support of the Burner Method

As discussed in Section 4.3, implementing the burner method in smoke plume models of type (A) requires the HRRPUA time history at computational grid cells on the terrain. The HRRPUA can be determined from the arrival time, residence time, and burning (or emission) rate. Overhead imagery has to potential to provide local estimation for these three quantities, but only at select time periods during large prescribed fires since the whole burn plot is not continuously observed. Below, sensor needs for the information required to obtain the HRRPUA are discussed.

Arrival time:
Fire front detection is usually based on infrared imagers; see Allison et al. (2016) for a review on airborne fire detection and monitoring. If only the arrival time at a location (i.e. detection of fire presence at a location) is required the use of low cost sensor based on Near Infrared (NIR), Short Wave Infrared (SWIR) or Thermal Infrared (TIR) is sufficient. However, TIR is certainly more suitable for intense fire, as NIR and SWIR can be blocked by smoke. Sensor saturation is not a problem here as we are only interested in detection. However, high frequency observation (high frame rate or high time resolution) is preferable, but not necessary if the fire front dynamics can be sufficiently estimated between observations (i.e. constant fire spread rate between observations exists).

Residence time:
A direct measure of the flaming residence time would require a TIR or Middle Infrared (MIR) sensor with a high frame rate, high spatial resolution, and no pixel saturation as: (a) fire depth needs to be resolved, and (b) temperature evolution at a pixel level needs to be analyzed and compared with expected flame temperature.

A workaround is to assume a constant fire front spread rate between observations, and use an instantaneous measure of fire depth (Fd) and rate of spread (ROS) to derive the residence time (Rt), Rt = Fd / ROS. The ROS can be derived using the spatial gradient of arrival time map (Paugam et al. 2013), while the fire depth can be estimated from TIR or MIR sensor with sufficient spatial resolution (~ 3 pixels span the fire depth) and large temperature sensitivity (high frame rate is not necessary here).

Fire depth:
Measures of fire front depth have received less attention than ROS, however several options exist. One is to use the potassium emission bands (766.5nm and 769.9nm) as described in Amici et al. (2011) or Vodaceck et al. (2002). This option has the advantage to lower the high spatial resolution constraint on the infrared sensor, but would require a multispectral sensor with a spatial resolution suitable to capture the fire depth along the whole fire front. Another option is

to use the dual-band approach of Dozier (1981). By combining information from TIR and MIR bands, the algorithm proposed by Dozier retrieves the size and the kinetic temperature of the black body that would have the same exitance. However, this won't give a direct measure of the fire depth only an area covered by the fire, and it is known that applying the Dozier algorithm at the pixel level has some limitations due to eventual misregistration between bands (Zhukov, 2006). Some geometric analysis would have to be carried along with this approach.

Emission Rate:
Emission rates are estimated from the emission factor and fuel consumption (Andrea and Merlet 2001). Emission factors are available in the literature (Andrea and Merlet 2001), while a map of fuel consumption can be estimated from the time integration of the Fire Radiative Power (FRP) product (Wooster et al 2005) which can be measured with a calibrated MIR sensor (Wooster et al 2005) or a TIR sensor (Hudack et al 2016). High temporal resolution is also required here unless the fire behavior can be assumed constant in between observations.

Challenges:
The main challenge of the overhead image processing is to quantify the effects the of sensor's frame rate and pixel resolution on the computation of the fire metrics introduced above, i.e. arrival time, fire depth, rate of spread, residence time and fuel consumption rate. Few datasets provide overhead or near nadir imagery with a sufficiently high frame rate and spatial resolution to support a sensitivity analysis of the influence of temporal and spatial resolution and the assumptions made regarding the fire behavior. Such datasets are necessary, for example, to validate the computation of fire behavior metrics from images collected with long return times (e.g. from satellites or air-borne platforms).

It is important to note that the calibration of overhead imagery (to obtain HRRPUA) using ground-based measurements requires that the fire seen by the overhead sensor coincides with the location of the ground instrumentation. Also, in order to have measures of uncertainty in the data derived HRRPUA multiple measurements under the same environmental condition are needed. This puts constraints on the field of view of the overhead imagery, frame rates, return times, and coordination with the ignition procedure which may not be achievable, especially for fires over large areas. For example, in the 703C fire, this occurred for only two of the ten ground based stations (Hudak et al., 2016(a)).

An effort is currently underway to create a pilot dataset from high resolution prescribed burns using three 7 ha plots that were burned in 2014 during an experiment conducted in Kruger National Park, South Africa. Two handheld cameras (TIR and MIR) were operated simultaneously from a helicopter hovering above the plot, offering a near-nadir platform. In such a configuration, imagery with a spatial resolution of ~1m and temporal resolution of 1 Hz (TIR) and 3 Hz (MIR) can be obtained. However, orthorectification of the imagery is much more challenging than when using a camera operated from fixed wing aircraft with an accurate Inertial Measurement Unit (IMU).

Together with the effect of sensor's geometry and spectral characteristics, the effect of flame lean, the vegetative canopy obscuration, and plume (e.g. water vapor, cloud water) absorption on the observed fire radiation should be considered.

Are measurements sufficient to implement the burner method for the 703C burn?

We now consider whether or not the measurements taken during the 703C burn could be used to implement the burner method. This fire was described earlier in Section 4.2 (see Figure 2). The imagery used here came from a TIR sensor operated in a fixed wing aircraft (Hudak et al. 2016(a)). The geo-referenced images have a resolution of 2.8 m and a time between observations which span from 5 seconds (overlapping images from the same aircraft transect) to 2 to 3 min (return time of the aircraft). At 2.8-m resolution, Figure 4 shows the raw arrival time map as extracted from the single frames, and Figure 5 shows the interpolated arrival time map assuming a constant ROS between observations.

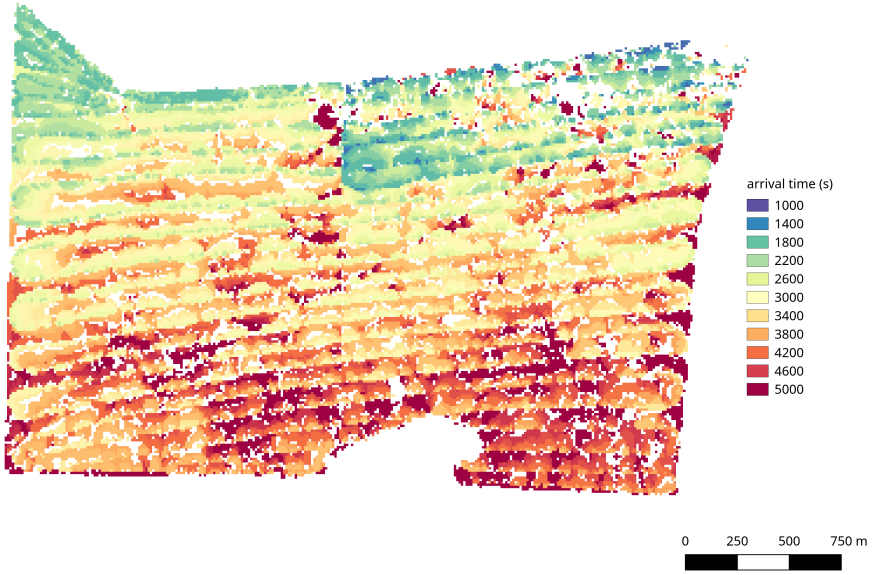

Figure 4: Fire front arrival time directly from imagery of prescribed burn 703C. Arrival time is shown as directly observed from the single overhead imagery available in the dataset. Since the whole plot is not continuously in the camera's field of view, some points on the ground are not observed when the fire is present. This is denoted by white pixels.

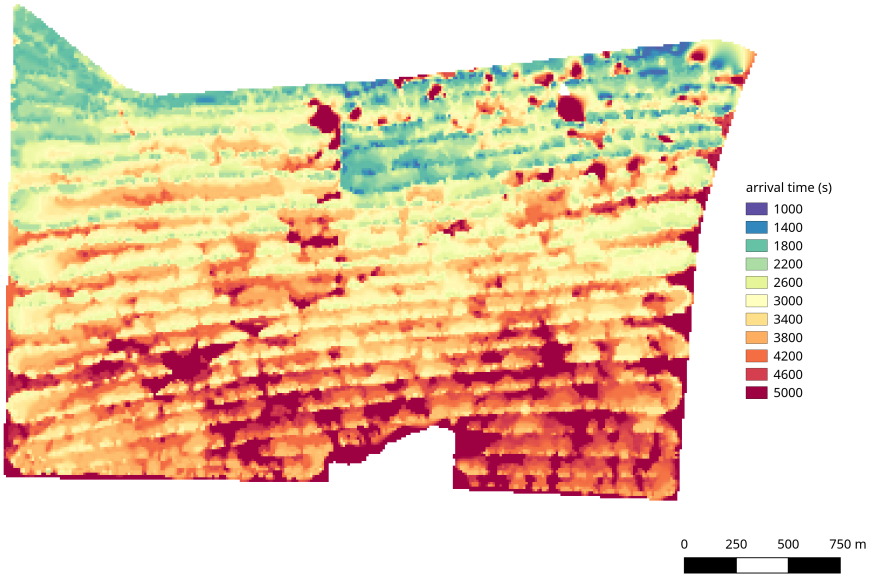

Figure 5: Fire front arrival time in prescribed burn 703C derived from interpolation. The interpolation is based on the more directly observed arrival times in Figure 4 and the assumption that the ROS is constant between observed arrival times.

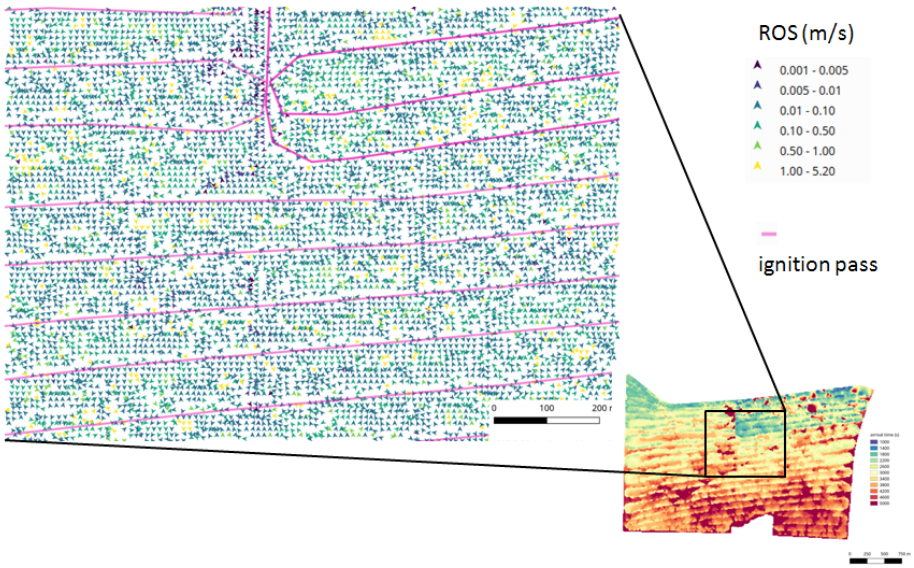

Figure 6: Map of derived ROS for prescribed burn 703C. The area shown is 800 x 1000 m^{-2} located in the center of the 703C plot as shown. ROS is computed from the interpolated arrival time map of Figure 5.

In the case of the 703C experiment, the coarse time resolution (2 to 3 minutes between flight overpass) was not too constraining on the arrival time map interpolation because the ROS was relatively low. However, the time resolution was low enough to prevent the computation of the residence time. For most of the pixels, the fire is only seen once or twice during the flame duration time, which is not enough to estimate a residence time and, therefore, HRRPUA.

The interpolated arrival time map is then used to compute the ROS, which is plotted in Figure 6. The results show a good match with ignition lines from the helicopter GPS (pink lines), in the sense that the ignition lines occur at locations with relatively few spread vectors. This demonstration shows that a calculation of the spread rate from overhead imagery is feasible. However, it is not known how accurate the ROS values are; more quantitative comparisons are required. It is possible that FASMEE could be an opportunity to run cross comparison of remote-sensing based approaches (such as the approach presented here) with ground-based in-situ measures of the ROS.

Given the ROS, the residence time could be computed from the fire depth. However, the fire depth for the 703C experiment is difficult to estimate. It is only possible to clearly identify the fire depth where it spans at least 3 pixels, which here represents a distance of about 9 m. The fire ignition procedure was designed to favor the propagation of many small, somewhat isolated fires, as seen on Figure 2. The 2.8 resolution of the LWIR sensor is only able to capture the flame front depth at the center of the larger fire "patches" with larger emissions (purple to pink color). This left many points with an unquantified fire depth which could, in sum, have a significant contribution to the overall HRR and, therefore, plume rise (see Section 4.5).

Regarding fuel consumption, Hudak et al (2016(a)) show that the spatial resolution and temporal resolution of the 703C was sufficient to compute map of Fire Radiative Energy (FRE) from time integration of FRP derived from the TIR sensor.

In summary, the data available for the 703C burn (TIR with a spatial resolution of 2.8 m and a time resolution <=2-3 min) is good enough to compute a map of arrival time, ROS, and fuel consumption. Further work is needed to develop a methodology for determining the uncertainty in these quantities. Also, the neither the fire depth nor residence time has been successfully estimated. Thus, the burner method could not be implemented without some assumptions or additional information. This points to the need for improvements in the sensors and/or the experimental design so that the fire depth and residence time can be determined for scenarios similar to burn 703C.

4.5. Demonstration of the Burner Method for a Spreading Fire

In this section, we give a demonstration of implementing the burner method in WFDS-LS by obtaining the necessary HRRPUA time history from a WFDS-LS simulation of a spreading fire. This approach could be used to assess the how different spatial and temporal resolutions of overhead imagery, which is used to derive the burners' HRRPUA, can impact the simulated smoke plume. As discussed above in the context of experiment 703C, there can be significant time periods with no aerial coverage (e.g., time intervals between image frames ranged from 5 s to 2-3 minutes). There are also other issues to consider, including limitations due to the size of a pixel on the ground, uncertainties in the calibration of the IR measurement data to obtain the HRRPUA, and the sensor's field of view, frame rate and return time. We do not address all these issues here. Instead, we choose to demonstrate, in a simple way, the sensitivity of the simulated smoke plume, using the burner method, to prescribed error in the HRRPUA that mimics poor spatial resolution in the IR imagery or poor calibration of the IR data to obtain the HRRPUA. The impact of poor time resolution is not considered, although it would be straightforward to do so.

The WFDS-LS model is implemented to create the "actual" fire. For simplicity, the fuel is chosen to be tall grass (height = 0.762 m, loading = 0.675 kg m^{-2}, surface-to-volume ratio = 4921 m^{-1}, packing ratio = 0.0017, moisture fraction = 0.06, char fraction = 0.2, heat of combustion = 18,000 kJ kg^{-1}). The ambient wind profile initially and at the inflow boundary, is $u(z) = 3(z/2)^{1/7}$ (m s^{-2}) and the lapse rate is LR = -6 C km^{-1}. The fire is ignited over a 4 m x 8 m area and spreads unhindered (no fuel breaks) on level terrain in a computational domain of dimensions 4.8 km x 2.4 km x 1.6 km; the grid resolution is 4 m. The simulated time is 20 minutes. The fireline develops into a head, long flanks, and a backing fire. This was desirable because it ensures that the HRRPUA varies along the fireline due to the changing fireline depth. The backing fire portion has the smallest fireline depth (~0.4 m) and HRRPUA (~60 kWm^{-2}) and the head fire the largest (~20 and 650 kWm^{-2}, respectively). This will allow us to modify the HRRPUA along the fireline based on a chosen cutoff on the minimum burner HRRPUA value. In this way, we mimic an IR sensor's non-detection or under prediction of the HRRPUA (note we could also test the impact of over prediction of the HRRPUA).

Figure 7 shows time history of the total HRR from a simulated fire. The results of four simulations are shown. During the WFDS-LS simulation, the HRRPUA of the fireline is output and then used as input for the other simulations to define the location and timing of the burners. Using the unmodified HRRPUA (denoted Burner in Figure 7) gives a time history for total HRR that's identical to WFDS-LS, as expected. In the burner simulation denoted HRRPUA >= 0.5 Max, a burner existed only if the HRRPUA at that location and time is greater or equal to half the maximum value possible (which is based on the fire residence time, loading, and heat of combustion). Similarly, in the simulation with HRRPUA=max, a burner existed at a grid cell only if the HRRPUA equaled its maximum value.

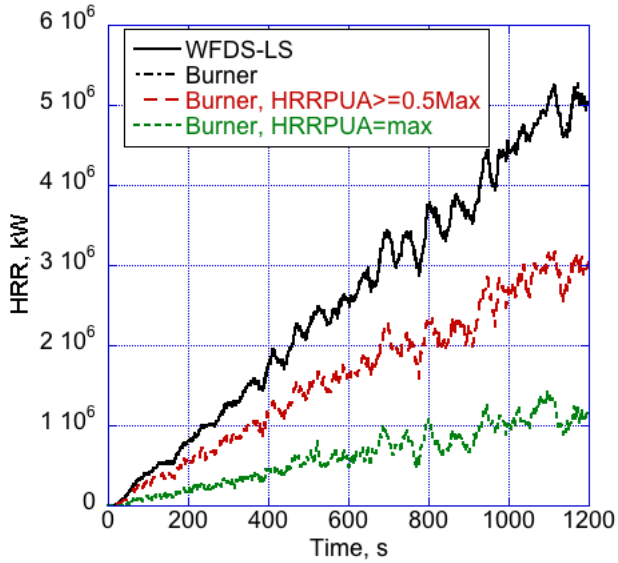

Figure 7: Time histories of the total HRR of a spreading fire using WFDS-LS or burners.

By imposing bounds on the HRRPUA we "turn off" portions of the fireline, starting with the backing fire and progressing through the flanks as the minimum cutoff is raised. This can easily

be seen in Figure 8 which shows the HRRPUA for the head and most of the flank portion of the fireline (i.e., the backing fire portion is not plotted) on the left and the resulting smoke plume on the right. Figure 7 and Figure 8 show that accurately measuring the top 50% of the HRRPUA along the fireline corresponds to 60% of the overall HRR and results in a simulated plume that reaches approximately 85% of the "actual" plume height. This stresses the importance of ensuring that the measurements accurately capture the highest HRRPUA values, since this portion of the fireline contributes disproportionately to the plume rise. The locations of ground based measurements for calibrating the overhead imagery derived HRRPUA should be chosen accordingly.

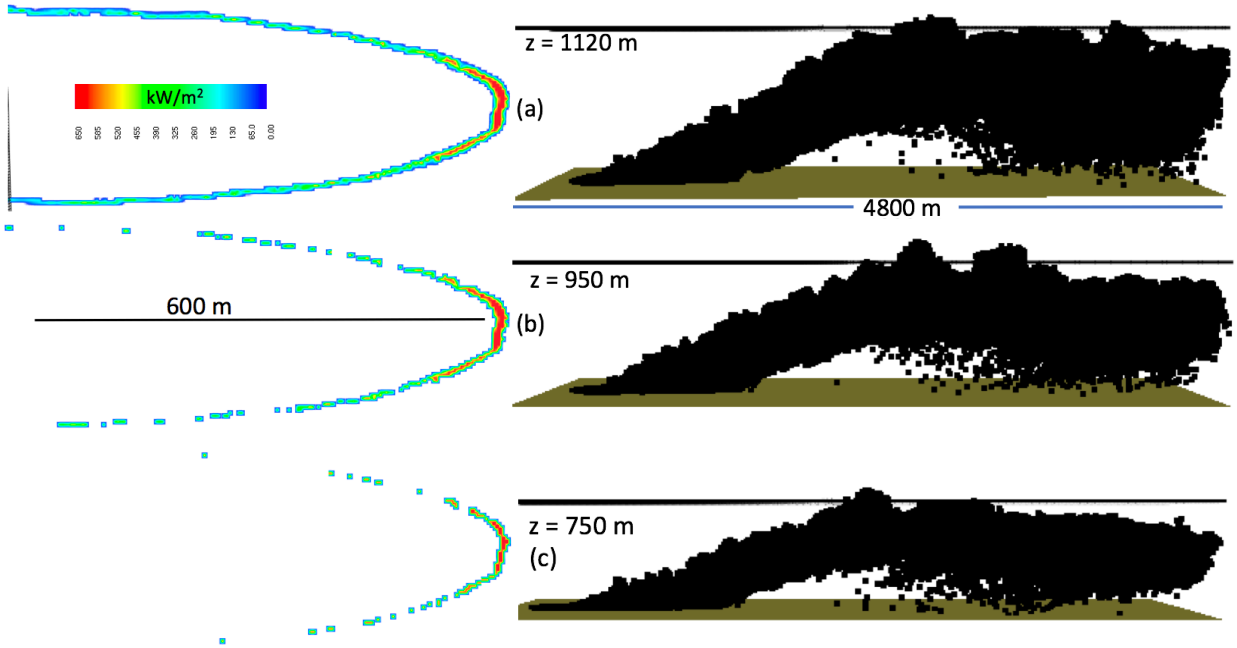

Figure 8: Fireline HRRPUA (left) and plume (right) from WFDS-LS and burner simulations. Fig. (a) shows the results of WFDS-LS; (b) WFDS simulation using burners with HRRPUA >= 0.5 HRRPUAmax; and (c) WFDS simulation with HRRPUA = HRRPUAmax. The loss of fireline as the minimum bound is raised is clearly seen in the figures on the left. The resulting loss in overall HRR (plotted in Figure 7) influences plume rise as see on the right-side figures.

The "spottiness" of the HRRPUA in Figure 8(b) and (c) is similar to the image of burning occurring in the field experiments shown in Figure 1 and Figure 2. In burn 703C (Figure 2), the spottiness could be caused by any combination of limited sensor threshold, variable vegetation, and local wind conditions, and the spot-like ignition procedure itself. The ignition procedures for the S5 and Camp Swift experiments (Figure 1) did not introduce spottiness; in those cases, it was vegetation driven.

4.6. Smoke Plume Simulations – Idealized Case using a Fixed Line-Fire Burner

Four models were applied to the simulation of a smoke plume created by a 750 m long stationary burner to represent a line fire. The depth (25 m) and HRRPUA (2000 kW m^{-2}) of the line fire is based on fires observed during the International Crown Fire Experiment (Stocks et al., 2004).

This fire is larger, in depth and HRRPUA, than most of the candidate FASMEE burns. However, it's depth is large enough that it physics based model WFDS-PB can be used. This allows a comparison between a model that resolves the combustion processes (WFDS-PB) to other models that do not (DaySmoke, MesoNH-ForeFire, WFDS-LS, WRF-SFIRE). Two ambient wind speeds as described by the vertical profile $u(z) = u_o(z/2)^{1/7}$ where $u_o = 1$ m/s or 5 m/s are used for the upwind boundary condition and initial condition. The lower wind case is a similar wind speed present in the RxCADRE 703C experiment discussed above (see Section 4.2). Also, for each u_o value, two lapse rates were used: LR = $dT/dz = 0$, -6 C/km. The surrounding terrain is level. The line fire is 500 m downwind of the inflow boundary. The computational grid resolution differs between models. For the atmospheric weighted models of MesoNH and WRF a 50 m grid cell resolution is used; and for DaySmoke a 200 m grid. WFDS-PB used a 5 m grid for a volume encompassing the fire line and near plume rise. WFDS-LS was run with two different resolutions: a fine resolution that matched the WFDS-PB simulations and a coarser resolution that matched the MesoNH and WRF simulations.

The WRF-SFIRE and MesoNH-ForeFire models have the ability to simulate more atmospheric microphysics (such as condensation). In order to have a more consistent comparison with WFDS, these microphysics models were not implemented. Differences between the models still remain, but the focus here was to simulate a basic scenario (but idealized, so lacking in some physics) in order to support a model comparison that was confounded by as few model differences as was reasonable.

Smoke plume cross-sections with gray-shading showing the vertical extent of the simulated plume, in a plane parallel to the ambient wind direction, are shown in Figure 9 ($u_o = 5$ m/s, LR = 0 C/km) and Figure 10 ($u_o = 1$ m/s, LR = -6 C/km) for models MesoNH-ForeFire, WFDS (fine grid only), and WRF-SFIRE. In all cases, the ambient wind flows from left to right. The modeled quantity used to produce the gray-shaded plume is not the same across models: soot density for WFDS-PB; number of Lagrangian tracer particles for WFDS-LS; passive scalar for MesoNH; soot density for WRF. Within the shading, a black line denotes the vertical centerline of the plume. The nearly vertical thinner black lines give a measure of the extent of the plume's cross-section perpendicular to the average convective flux, $\vec{F} = \rho c_p (T - T_o)\, \vec{u} \cdot \hat{n}$ (GW), where $\hat{n}$ is the unit normal in the direction of the average flow velocity through the cross-section. Arrowheads point in the direction of $\vec{F}$ and their colors show the magnitude of $\vec{F}$ in the order of blue-green-yellow-orange-red denoting the range 0 to 40 GW.

Figure 11 and Figure 12 are plots of the centerline plume height for all the models. In these plots the results of DaySmoke are also included. DaySmoke is the simplest of the models considered and operates by representing the flaming area as a circle with the equivalent area. For the 25 m x 750 m line fire this is a circle with a 155 m diameter. The DaySmoke plots correspond to this area. Increasing this area will raise the plume height.

The main points of interest regarding Figure 9 through Figure 12 follow. Note that the generality of the following findings is not known. This is because the simulations covered a very limited range of conditions, have an idealized heat source, and no detailed investigation into the relevant difference between the models was undertaken.

1) It's possible to implement the burner method in a range of smoke model types.
2) Across all wind and lapse rate conditions:
   a) WFDS-PB and WFDS-LS agree, suggesting that explicitly resolving the combustion physics is not necessary for smoke plume focused simulations if the HRRPUA is known.
   b) The downwind distance at which plume stabilization occurs is very similar across models, except for DaySmoke which reaches neutral buoyancy sooner.
   c) The predicted far-field plume heights are consistent across models. The one exception to this is MesoNH-ForeFire which has a higher plume height in the $u_o = 1$ m/s, LR = -6 C/km case (see Figure 12).
   d) The plume rise centerline predictions definitely differ most between the models. This points out the need for measurements that will support the identification and improvement of the physics-based sub-models that handle the processes involved in the interaction of the ambient and buoyancy generated wind fields during plume rise.
3) For the high wind cases, the vertical extent of the plume far downwind differs between the models (see Figure 9). This has important implications to the predictions of smoke at ground level. This points out the need for measurements of ambient atmospheric turbulence, which drives dispersion of smoke particulate at these distances from the fire.

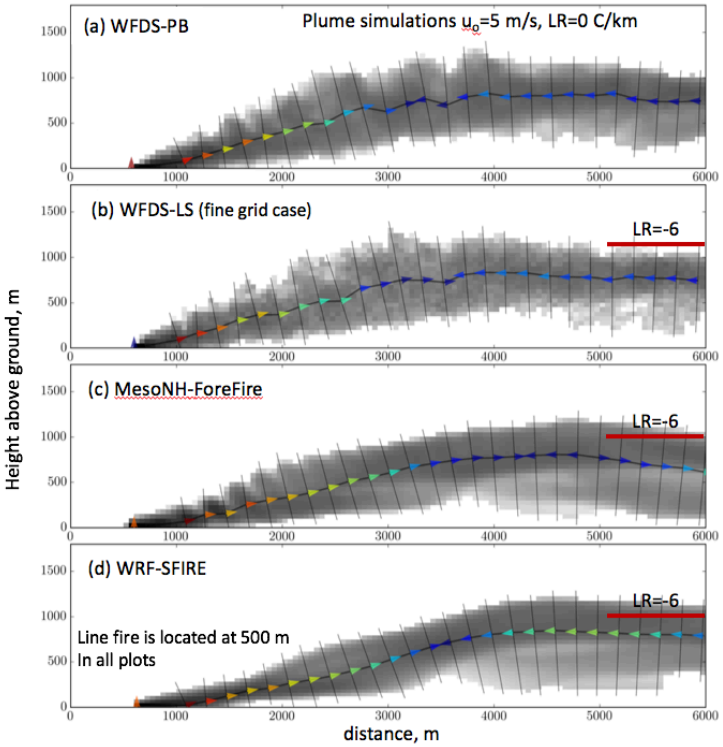

Figure 9: Simulated smoke plumes from a line fire (u_o= 5 m/s, LR = 0 C/km).
Cross sections of plumes are shown at time t = 1000 s after ignition of the stationary line fire. Results from four models are shown. The combustion processes are directly modeled by WFDS-PB in Fig. (a). The other models shown in (b) – (d) do not explicitly model combustion. The thick magenta line on the right-hand-side of Figs. (b) – (d) shows the plume center height at distance 6000 m for the case of LR = -6 C/km.

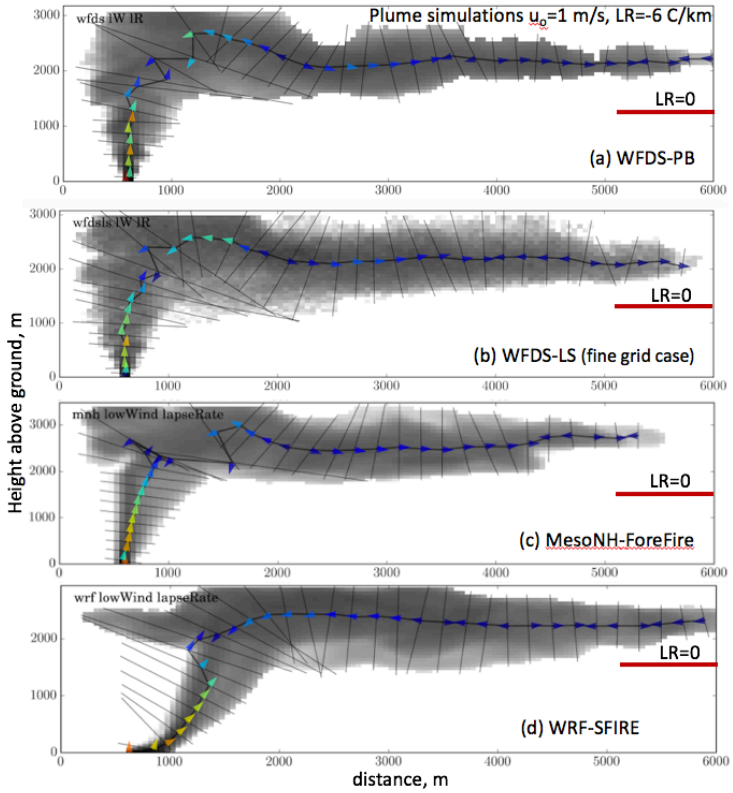

Figure 10: Simulated smoke plumes from a line fire (u_o= 1 m/s, LR = -6 C/km).
The same quantities as in Figure 9 are plotted also at t = 1000s, but for the lower wind speed case. Also, note that unlike Figure 9, in this figure the shading, centerline, and convective flux are for a lapse rate of -6 C/km, not LR = 0 C/km. Compared to the higher wind case, the plume rise significantly higher and the difference in height between the LR = 0 C/km versus LR = -6 C/km is greater.

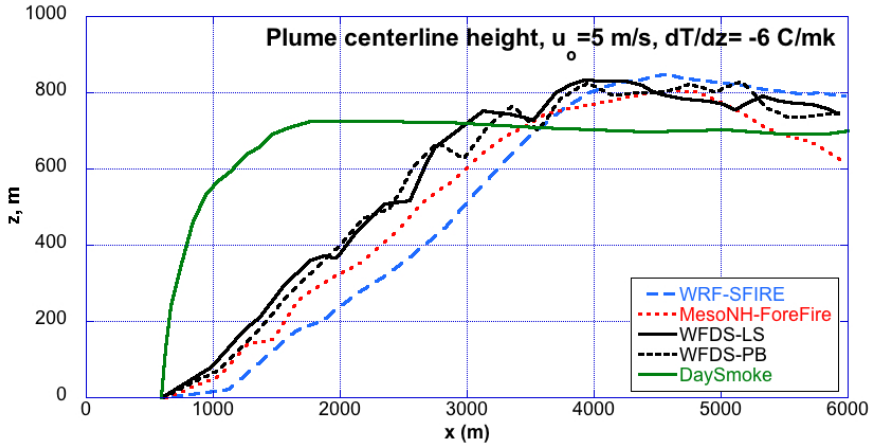

Figure 11: Plume centerline location for the u_o= 5 m/s, LR = 0 C/km, case.
This is the case for which plume cross-sections are plotted in Figure 9. The two WFDS implementations agree with each other. All models reach a stabilization height, $z \approx 4000$, at $x \approx 4000$ m. The largest difference between models occurs during plume rise.

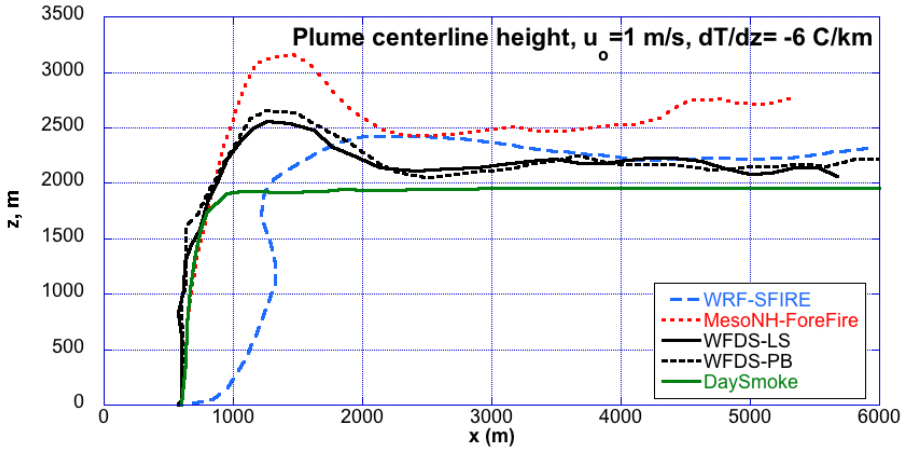

Figure 12: Plume centerline location for the u_o= 1 m/s, LR = 0 C/km, case. This is the case for which the plume cross-sections are plotted in Figure 10.

4.7. Simulations of Fire on an Isolated Hill

For the purpose of exercising both model set up procedure and gaining perspective on possible issues with simulating FASMEE burns, FIRETEC was used to perform simulations of the proposed burning of a "knob", which is a ~800 m diameter dome shaped terrain feature at the Fishlake burn site (-112.086997, 38.434705 Decimal Degrees). This knob was chosen based on its tractable size and the fact that one of the postulated ignition methods was to "ring" the knob. The resulting fire-induced winds could result in fireline acceleration thereby increasing the fire depth and reducing the influence of vegetation inhomogeneity. In addition, a well-defined plume would develop. Overall, this scenario could result in easing both measurement and simulation challenges. However, the object of this exercise was not to perfectly simulate a proposed fire (as the details of this fire have not been worked out and in fact, this fire might not even happen), but more to gain perspective and demonstrate what was required in terms of assumptions or input data for simulation of such a burn and develop an early set of lessons learned.

For this exercise of simulating a ring fire of the knob, a 1.5 km x 1.5 km computational domain with 2 m horizontal resolution was selected based on its computational tractability, resolution sufficient to capture some of the vegetation heterogeneity and the fact that it provided approximately a 200 to 300 m buffer between the knob and the domain boundaries. The first lesson that is illustrated by this exercise is that this size of buffer might not be sufficient, especially in the context of this rugged terrain.

Susan Prichard and Benjamin Bright used ArcGIS software to generate topography and vegetation class maps as a rasterized set of altitudes at 2 m resolution. The topography was taken from 10-m National Elevation Dataset (NED) and the vegetation class map was provided by LandFire. Given the rasterized fuel classification map with 3 dominant fuel classes, Subalpine Fir - Engelmann Spruce - Douglas-fir - Lodgepole Pine Forest (FBFM9 and FBFM10); Trembling Aspen Forest (FBFM2 and FBFM8); and grassland as well as barren ground, such as roads (Figure 13), the next step was to populate the FIRETEC computational cells with an appropriate bulk density, surface area per unit volume, moisture and vertical distribution for the fuels. For the actual burn site, the average load, height, moisture, and surface area per unit

volume would be known for the typical grass and hopefully for specific regions in the domain. These values can be used to specify the fuel in the surface layer for the cells in regions where the fuel class is grass.

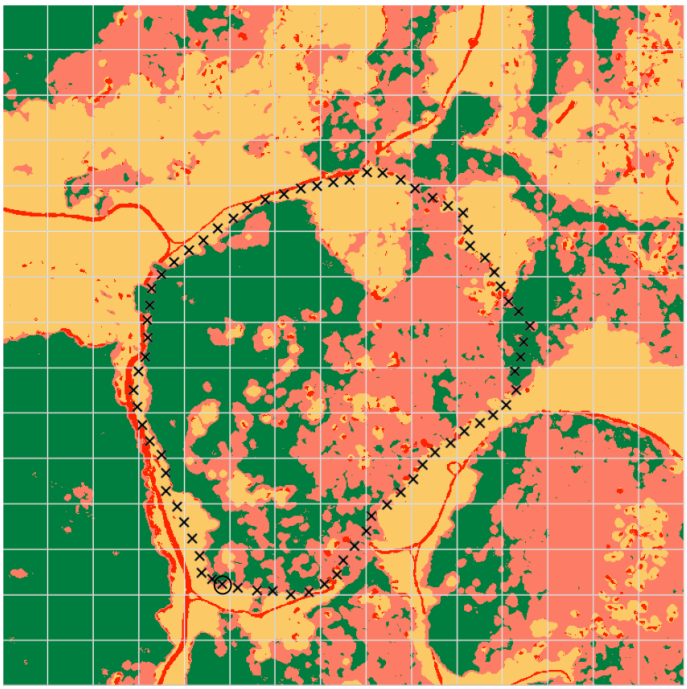

Figure 13: Fuel map for FIRETEC simulation of hypothetical ring fire on knob at Fishlake.

Different colors are used for each fuel class and representative tree species used for populating fuel for FIRETEC: green Douglas Fir forest (for FBFM9 and FBFM10), pink indicates Aspen forest (for FBFM2 and FBFM8); yellow indicates grassland; and red indicates barren which is mostly roads at the site. The black X symbols indicate aerial ignition sphere locations. The circled X indicates the first ignition sphere for the case with westerly wind shown in Figure 14 and Figure 16. Subsequent ignitions progress sequentially in a counter clockwise direction. The overlaid grid demarks 100 m distances and the domain is 1.5 km x 1.5 km

In the regions where tree crowns are present, various possible approaches can be applied for populating fuels in FIRETEC cells. The simplest is to specify a homogenized fuel layer using average canopy bulk density, height to live crown and any vertical distribution information that is available. Unfortunately, past studies show that this approach is not necessarily adequate when as the crowns of trees have larger separation distances from one another as the canopy discontinuities inhibit crown fire spread and local bulk densities tend to be significantly different from the mean bulk density. A second possible to place virtual trees based on knowledge or assumptions about the distributions of trees. Extremely high-detail data sets might include stem-mapped trees with height-to-live-crown, tree height, tree diameters, tree bulk densities. This would be an extremely rare level of detail given current data collection techniques, but developing LiDAR techniques might provide this high level of detail in the future.

In the absence of very high-detail data, there could be data sets of statistical distributions of trees from which virtual trees can be chosen or lists of trees that are representative of the site. Other

methods include referencing standard distributions for a tree type or a tree list of representative tree species from a forest in another location. Given one of these methods of specifying trees, a methodology such as described in Linn et al. 2005 can be used to generate a virtual forest. Additional information such as local aggregation (are the trees randomly spaced or concentrated in patches) can be used to further refine the generation of the virtual forest if available. Luckily several of the FASMEE sites (at least the western sites) have high tree densities and patchiness is not a dominant characteristic. In the regions that have tree species, information to specify surface fuel including litter and grasses is also needed to populate the values for the ground cells both under trees and in openings if they exist. This can be done by uniformly distributing litter/grass mass on the landscape or making a function of the canopy overstory such as done in Linn et al 2005.

For this exercise, we populated the trees based on datasets measured in the Douglas Fir forest (representative species for FBFM9 and FBFM10) and Aspen forest (representative species for FBFM2 and FBFM8) near Las Vegas and Gallinas, New Mexico.

Regarding wind information, ideally we would like to have initial conditions throughout the domain and boundary conditions for the duration of the fire at the grid resolution of the model. As discussed in Section 4.1 for large experimental sites such as FASMEE, it is nearly impossible to measure winds at this level of detail. Even for "well-instrumented" (see Section 4.1) experiments assumptions and estimates are required on the part of modelers to define the initial and boundary conditions for computational domains. To further complicate things, the influences of the unmeasured winds depends heavily on the nature of the fire as explained above. Some researchers have estimated that the scale of the turbulence that is important goes with the depth of the flame zone. One possible advantage of a ring fire scenario is that fireline acceleration will increase the fire depth sufficiently to make the unmeasured details of the wind irrelevant.

For this exercise, there is no wind data because the burn has not occurred yet and thus a simple idealized mass conserving terrain specific velocity field was used for the initial velocity field in the domain and for prescription of the boundary conditions throughout the simulation. Simple background height-dependent velocity fields were specified for several different simulations and these background winds were then adjusted for topography and mass consistency. The winds are then allowed to evolve in FIRETEC and come to a balanced topography and vegetation dependent state throughout the domain before the fires are ignited. Due to lack of knowledge concerning any evolution in the velocity field during the burn, the boundary condition winds were assumed to be constant and no prescribed velocity fluctuations were specified, which would be different if actual wind data were available. Two of the wind fields resulting from adjustments due to complex topography and heterogeneous vegetation with background velocity (initial and boundary conditions) profiles based on $1/7^{th}$ power-law, with 6 m/s of wind speed with the references height of 10m are shown in Figure 14, for westerly winds (blowing from west) and Figure 15, for southerly winds (blowing from south). This methodology is easy implement and probably served the purpose of this exercise, however, it has a potentially serious drawback in which the velocities prescribed at the boundaries do not reflect the surrounding topography that exists outside of the selected domain. The significance of the errors caused by ignoring surrounding (especially upwind) topography will depend on the wind speed direction

and of course topography. Although it was outside the scope of this current exercise, future more-extensive efforts to refine such exercises would be advised to use lower-resolution LES calculations (potentially using a model such as WRF-LES) to obtain dynamic heterogeneous boundary conditions that are more consistent with surrounding topography.

The next aspect of the burn that must be accounted for is any areas that are blackened before the field experiment. These features are relatively easy to handle in models such as FIRETEC or WFDS by simply removing surface and ladder fuels for low intensity pre-burn treatments or removing all fuel in regions with high-intensity pre-burn. Treating the blackened area appropriately in the model impacts both the fires ability to spread into those regions and also impacts the air flow around the fire.

Fire behavior can be very sensitive to fire ignition patterns and the rate at which the patterns are deployed on the landscape. In the case of aerial ignitions, this translates to the locations of the ignition spheres and the rate at which they are laid down. This can be translated to a flight path flight speed and rate of ignition sphere release if we assume that ignition spheres are dropped vertically. If they do not fall vertically then this should be compensated for in the location of the spheres relative to the flight path. For this FIRETEC exercise of simulating a ring fire on one of the knobs at Fishlake, a hypothetical aerial ignition pattern was selected based on suggestions by prescribed fire aerial ignition experts, shown in Figure 2. This flight pattern was generated based on the idea that a helicopter would fly around the base of the knob as a speed of 40 knots (21 m/s) and ignition spheres are dropped ~130 feet apart (~39 m). It takes 135 seconds for the ignition circle to be complete. In FIRETEC, the time it takes for the ignition fires to grow from the size of an ignition sphere to a resolvable size (~ 4 m in diameter) is taken to be a constant for all of the ignition locations. This time delay is inherently built into the simulations such that it has already occurred when fires develop in the simulation.

The presence of complex terrain and heterogeneous vegetation can create complex wind fields near the ground. As a result, different flight paths for aerial ignition, which results in different distributions of ignition spheres, could result in significantly different fire behavior, at least initially. For example, Figure 14 and figure Figure 15 show the streamwise wind velocity components (U for Figure 14 and V for Figure 15) at 1.5 m above the ground prior to the start of the fire. In both cases, local winds that go against prevailing wind direction are observed near the ground at some locations. These plots illustrate the heterogeneity of the wind field and the location of the ignition spheres can determine the wind environment they are exposed to.

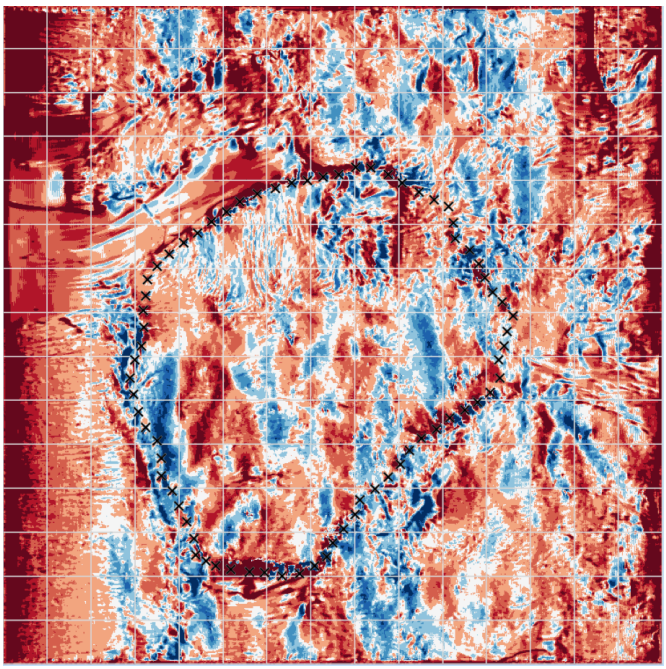

Figure 14: U (west to east) component of the winds at 1.5 m above the ground. Prevailing wind direction is westerly. X's indicate the aerial ignition sites. Red indicates positive (westerly) wind speed in x-direction, blue indicates negative (easterly) wind speed. Each color indicates changes in wind speed of 1 m/s, thus darkest red indicates above 4.5m/s, thus darkest blue indicates below -4.5m/s, while white indicate wind between -0.5 and 0.5 m/s.

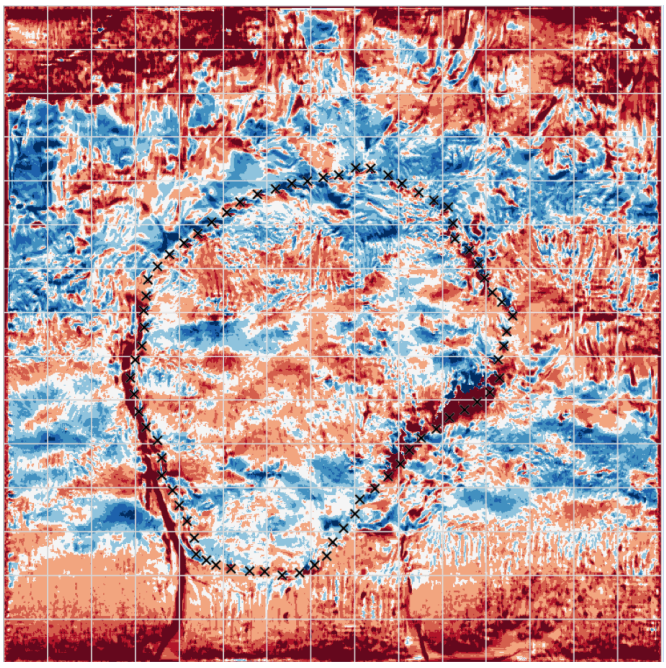

Figure 15: V (south to north) component of the winds at 1.5 m above the ground. Prevailing wind direction is southerly. X's indicate the aerial ignition sites. Red indicates positive (southerly) wind speed, blue indicates negative (northerly) wind speed. Each color indicates changes in wind speed of 1 m/s, thus darkest red indicates above 4.5m/s, darkest blue indicates below -4.5m/s of wind speed, while white indicate wind between -0.5 and 0.5 m/s.

Once the ignitions were started the simulations (first ignition is done at 15 seconds after simulation and it took 135 seconds to complete ignition process) were allowed to progress for 990 s. The progression of the fire that resulted from the wind fields shown in Figure 14 is illustrated in Figure 16. The panels in Figure 16, which are 150 s apart show the progression of the fire including the counterclockwise ignition progression, the growth of some of the ignitions to spreading fires, the acceleration of some of those fires (in both desired and unexpected directions). Some of the ignitions did not result in spreading fires, but some of them resulted in intense spreading fires.

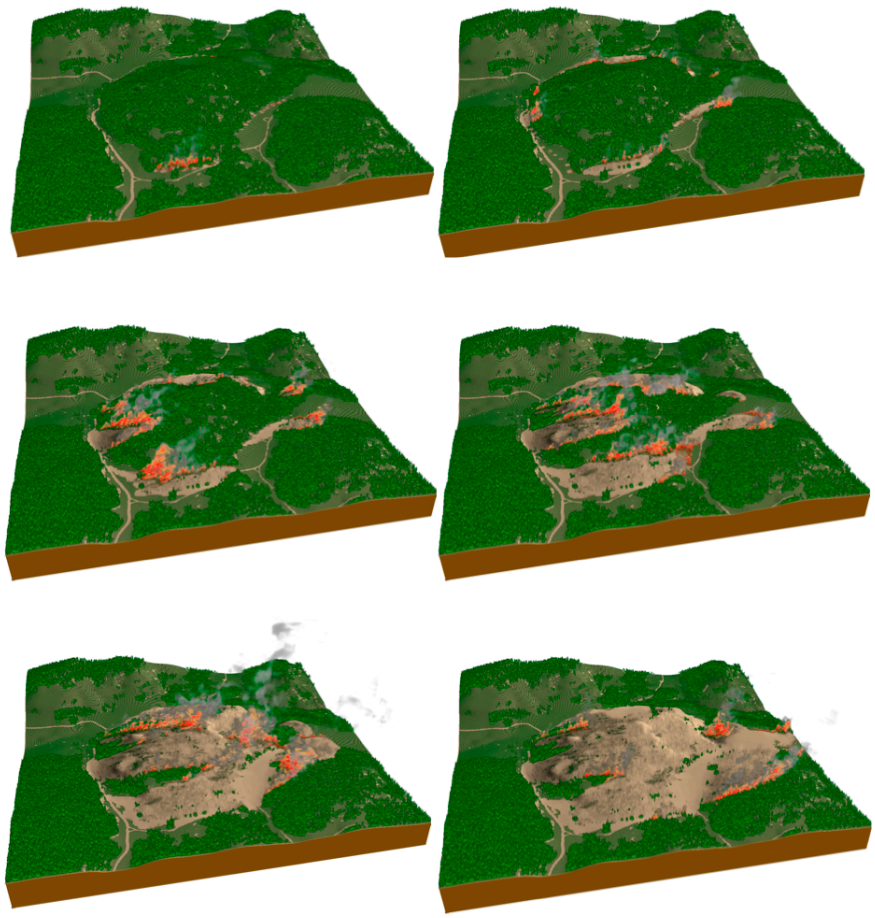

Figure 16: Visualization of a FIRETEC simulation of Fishlake site.
Ambient winds were westerly, 6m/s wind at 10m height. Fire progression at 150 sec (when the ring ignition is completed), 300sec, 450sec, 600sec, 750 sec and 900sec after the simulation started are shown in six panels.

This simulation resulted in some facets of fire behavior that were as expected such as fire runs uphill from various directions, but it also resulted in some fire behavior that was not expected. For example, the segment of fire on the upwind (west or left in the images) side of the ring that does not run up the hill, even though the prevailing mean wind is in this direction. By looking at the wind field map (Figure 14), it can be seen that even though the mean wind is left to right (west to east) in this simulation, the topography/vegetation-influenced flow is very slow or even east to west at this particular point. Additionally, the fact that some of the estimated positions of

the ignitions relative to the hill slope on the downwind side of the knob might have been unrealistic or certainly less than optimal (maybe they should have been more on the hill slope) and the lack of blacklining on the downwind (east) side of the knob led to the fire moving downwind instead of moving up the slope of the knob. Due to the spacing between the ignition points, the time that it took to circle the knob, the fuels along some portions of the perimeter and the topography/fuels induce flow fields, the ring became broken in several locations and did not form the desired continuous ring fireline. The result was that this ignition pattern did not lead to the widespread stretching out of the flame zone that was desired. This could be an artifact of the details of how individual ignitions were implemented in the code and their susceptibility to going out (this is largely a subgrid-scale process for FIRETEC simulation with this resolution) the type or conditions of the fuel they landed in given the heterogeneous winds, or the maybe the single circle of balls 130 feet apart might not be realistic for this type of firing operation in these sorts of fuels. Regardless, it points out the importance of representing the ignition process the heterogeneous winds and surface fuels appropriately as the resulting fire behavior can be very sensitive to it. If this simulation is accurate, then it might suggest the need for higher density ignition points around the perimeter or even an ATV ignition.

In these FIRETEC simulations, the thick woody material and any possible smoldering of duff was not simulated. Capturing these longer time-scale effects for smoke production purposes could be done through parameterizations, but would require greater knowledge of the moisture profiles within the thick fuels and duff layers. The result of this simplification is not expected to be significant in terms of fire spread but could be significant in terms of the sustained smoke production depending on the moisture levels and fuel loads.

4.8. Field Measurement Needs

The measurement needs of WFDS-LS, which has a simple fire front propagation model, are very similar to WRF-SFIRE and thus are not listed here since they can be found in the final report for the FASMEE Phase1 WRF-SFIRE project (Kochanski 2016). Below, the additional modeling needs for FIRETEC and WFDS-PB are listed. Some of the measurements listed below are also needed to implement the burner method as was discussed above.

1) Ignition Procedure
   a) Timing and location of ignition source: Required measurements are 1) the location on the ground of ignition sources (“ping pong balls” or other sources), 2) the time these sources were placed on the ground, and 3) the time needed for an ignition to grow to a fire of the same size and intensity as the measurement resolution (e.g., thermal energy). If these quantities cannot be determined, then some estimate of them will be needed, which will require exploration of the sensitivities to such estimates. This information will help both to implement the burner method and to initialize models that simulate the spread of the fireline.
2) Fuel
   a) Basic fuel properties: In order to provide information for a range of fire behavior models the usual fuel properties are needed: char fraction, moisture fraction, fuel loading, height, surface-to-volume ratio. These may depend on fuel type.
   b) Fuel consumption: The rates at which fuel mass is consumed is a critical measurement for implementing the burner method because it is directly related to the heat release rate and

moisture vapor creation. The rate of fuel consumption needs to be correlated with overhead imagery of the fireline. This will require ground-truthing and is a significant effort in itself.

c) Spatial fuel heterogeneity: Ideally, the rate of fuel-mass consumption will be robustly related to the overhead imagery of the fireline. If this is the case, then the influence of spatial heterogeneity in the vegetation will be accounted for implicitly. However, measures of spatial heterogeneity in the vegetation may be required to develop the relationship between overhead imagery and rate of fuel-mass consumption. This measure may be relevant if the spatial heterogeneity of the fuel occurs on the scale of the overhead imagery pixels. Estimates are probably also necessary for the three-dimensional fuel structure and nominal heterogeneity of the pre-fire stand. Some estimate is also needed of the stand structure that remains after the fireline passes, because this estimate determines the drag and thus could affect the indrafts and plume velocities near the ground, especially for lower-intensity fires. The raised vegetation can also obscure the detection of the radiative emission from the fireline as seen from the airborne sensors. For this reason, measures of the spatial distribution of vegetation between the fire and the overhead thermal radiation detector are needed.

3) Fire Behavior and Heat Release
   a) Estimation of the fire heat release: The fundamental quantity needed to implement the burner method is the time-dependent and spatially-explicit heat release rate per unit area throughout the burning domain.
   b) Representation of the heat transport from fire to atmosphere: The need for this measure is similar to that for WRF-SFIRE. Measures of heat transport with a vertical component would help to evaluate and improve the model. Estimates are needed of the fraction of the heat release that is transported by radiation and the fraction of the energy that is absorbed by the gas phase and convected upwards.
4) Plume development and meteorology
   a) Representations of local flow and fire-atmosphere feedbacks: This measurement is needed for the same reasons listed in the WRF-SFIRE model needs.
   b) Impact of turbulence on pyro convective updrafts: Needed for the same reasons listed in the WRF-SFIRE model needs.
   c) Importance of model resolution relative to fire size: Needed for the same reasons listed in the WRF-SFIRE model needs.
   d) Atmospheric boundary conditions: These needs are the same as those for WRF-SFIRE. These boundary conditions can also be obtained from WRF simulations.
   e) Background atmospheric turbulence. This is especially important in regions downwind of the fire where the plume has reached neutral buoyance. Is such regions, smoke movement in a direction other than that of the mean flow is through turbulent dispersion (e.g., this is how the smoke reaches the ground from above).

4.9. Integrated Data Management Needs

To date, no field measurement campaign, whose objective is to support the next generation of physics-based fire and smoke behavior models, has produced an integrated, co-located in space and time, publicly available and documented set of products representing data collected for the entire campaign. This has contributed to the paucity of next generation fire and smoke modeling

validation efforts. There are, however, a disproportionate number of efforts to advance individual measurement science disciplines and techniques from these fields campaigns.

Implementing the burner method and developing and validating the next generation of physics-based models for fire behavior and smoke will require field data across a range of spatial and temporal scales detailing environmental conditions, and fire and smoke behavior information. These data sets must be interpretable and distributable to an audience beyond those involved in the field campaign, ideally to future audiences who are not part of the measurement campaign. Efforts to qualify, quantify or otherwise describe as practical uncertainties within and between data sets are essential to both short-term and long-term use of this data.

In addition, currently available data is not assessed for uncertainty between data sets in space and time, and integrated and interdisciplinary efforts remain elusive. Many of the shortcomings of historic field campaigns are a result of insufficient data management and lack of standards related to geospatial science and technology (GSAT) employed in these campaigns. For example, no field campaign to the authors' knowledge has made an attempt to calibrate all data against a consistent temporal standard. Finally, the need for formal incorporation of GSAT in the study of WUI and wildland fire environments has been identified through federally funded research efforts (McNamara et al, 2016).

GSAT, integrated with current best practices in data management, inherently supports and, when done properly, demands appropriate integration and assessment (in time and space) of field measurements. The need for this cannot be overemphasized. Since a main objective of FASMEE is to support the testing and development of next generation smoke models (even if only to improve simpler operational models), the use of current GSAT and data management practices is essential to FASMEE's success and for legitimately setting an example of how complex, multidisciplinary measurement efforts can be successfully *interdisciplinary* in practice and outcome.

The development of an integrated data management plan was funded in the Phase I effort and a report was submitted to FASMEE leadership (McNamara, 2017). This report provides a framework for establishing the use of GSAT and sound data management practices to ensure that the FASMEE effort results in measurements that are integrated (in space and time), assessed for quality, and made publicly available in a reasonable time period. The report also discusses many other important topics to be addressed, including (but certainly not limited to) the uncertainty in the data, data quality assurance, and spatiotemporal data standards. We strongly encourage the JFSP governing board and FASMEE leadership to recognize GSAT as a required discipline for efforts such as FASMEE and provide appropriate funding and support. We believe this support will be essential to producing co-located, multi-scale measurements of pre-fire fuels, active fire processes, and post-fire effects required to begin to tackle fundamental fire science questions.

5. Conclusions

Based on a number of factors (including the expected fire behavior, plot size, ping pong ball ignition procedure, and the outcomes of past field experiments) the proposed FASMEE burns with low to moderate fire intensity are not suitable for a measurement effort whose goal is the

creation of validation data sets for physics-based fire behavior models. The exception to the above would be well-behaved fires with fire front depths in excess of 10 m and a well behaved simple ignition procedure such as a single line ignitions. While this may be possible for one or two FASMEE burns, it this is not representative of a typical prescribed. Validation of fire behavior models is lacking, especially for complex dynamic fire behavior that results from ping pong ignition procedures. For this reason, a smoke plume simulation that uses a fire behavior models, whether physics-based or not, will introduce unquantified errors into the plume simulation.

It is possible to provide the necessary observations to run and test the next generation smoke models while not explicitly simulating fire behavior. This requires measurements that define the HRRPUA along the fire front and is called the burner method. The burner method was successfully implemented in five different smoke plume models. Comparison of the resulting model predictions show the need for measurements of plume rise and far field smoke transport. The full suite of supporting measurements needed to implement the burner method across the large plots of interest in FASMEE are wanting and development and testing is needed. If the burner method is adopted, then high resolution ground measurements should be focused on supporting its implementation. Preliminary simulations suggest that it is important to quantify are the higher magnitude HRRPUA areas since these may have a disproportionate influence on smoke plume rise (although this will depend on the distribution of HRRPUA over the fire front). Preliminary simulations of an isolated hill suggest that, in complex terrain, fire behavior may be more sensitive to the details of the ignition pattern.

It is critical that design and implementation of the field experiments be conducted within the supporting framework of geospatial science and technology practices. If this is not done, FASMEE is likely to result in a set of disjoint, nonintegrated, datasets that will hinder their wide use by the scientific community of interest.

Table 1: Project deliverables

Deliverable	Description	Date
Project kick-off meeting	Participated in a 2-day planning retreat, Seattle	April, 2016
SW reconnaissance field work	Participated in a field tour of the Fishlake and Kaibab/N Rim study sites	July, 2016
Observational study design	Contributed to the FASMEE Study Plan, the main deliverable of Phase I.	March, 2017
JFSP Final Report	Final report (this document)	June, 2017

Literature Cited

Achtemeier GL, Goodrick SA, Liu Y 2012 Modeling Multiple-Core Updraft Plume Rise for an Aerial Ignition Prescribed Burn by Coupling Daysmoke with a Cellular Automata Fire Model. *Atmosphere* **3**(3):352-376.

Andreae MO, Merlet P 2001 Emission of trace gases and aerosols from biomass burning, *Global Biogeochem*. Cy., **15**, 955–966

Allison RS, Johnston, JM, Gregory C, Sion J 2016. Airborne Optical and Thermal Remote Sensing for Wildfire Detection and Monitoring. *Sensors* **16**:8

Amici S, Wooster MJ, Piscini A 2011 Multi-resolution spectral analysis of wildfire potassium emission signatures using laboratory, airborne and spaceborne remote sensing, Remote Sensing of Environment, **115**(8) pp. 1811 - 1823. DOI: 10.1016/j.rse.2011.02.022

CMAQ 2017 https://www.cmascenter.org/cmaq/

Bova A, Mell W, Hoffman C. (2015) A comparison of level set and marker methods for the simulation of wildland fire front propagation. *International J. Wildland Fire* **25**(2): 229-241

Dozier J 1981 A method for satellite identification of surface temperature fields of subpixel resolution, Remote Sens. Environ., **11**,221–229, doi:10.1016/0034-4257(81)90021-3

Filippi, JB, Bosseur, F, Mari, C, Lac, C, Le Moigne, P, Cuenot, B, Veynante, D, Cariolle, D and Balbi, J-H 2009. Coupled atmosphere-wildland fire modelling. *Journal of Advances in Modelling Earth Systems* **1**, 11.

Hiers JK, O'Brien JJ, Mitchell RJ, Grego JM, Loudermilk EL 2009. The wildland fuel cell concept: an approach to characterize fine-scale variation in fuels and fire in frequently burned longleaf pine forests. *International Journal of Wildland Fire* **18**: 315-325.

Hudak AT, Dickinson MB, Bright BC, Kremens, RL, Loudermilk EL, O'Brien, JJ, Hornsby BS, Ottmar RD 2016(a) Measurements relating fire radiative energy density and surface fuel consumption - RxCADRE 2011 and 2011, International Journal of Wildland Fire, **25**: 25-37.

Hudak, Andrew T.; Bright, Benjamin C.; Kremens, Robert L.; Dickinson, Matthew B. 2016(b). RxCADRE 2011 and 2012: Wildfire Airborne Sensor Program orthorectified and calibrated long wave infrared images. Fort Collins, CO: Forest Service Research Data Archive. https://doi.org/10.2737/RDS-2016-0007

Hudak, Andrew T.; Bright, Benjamin, C.; Satterberg, Kevin L. 2016(c). RxCADRE 2008, 2011, and 2012: Lidar data and derived raster products. Fort Collins, CO: Forest Service Research Data Archive. Updated 08 September 2016. https://doi.org/10.2737/RDS-2015-0010

Hudak, Andrew T.; Bright, Benjamin C.; Dickinson, Matthew B.; Satterberg, Kevin L. 2015. RxCADRE 2008, 2011, and 2012: Radiometer locations. Fort Collins, CO: Forest Service Research Data Archive. https://doi.org/10.2737/RDS-2015-0035

Hudak, Andrew T. 2014. RxCADRE 2008, 2011, and 2012: Ground cover fractions. Fort Collins, CO: Forest Service Research Data Archive. https://doi.org/10.2737/RDS-2014-0029

Hudak, Andrew T.; Bright, Benjamin C. 2014(a). RxCADRE 2008, 2011, and 2012: Clip plot locations. Fort Collins, CO: Forest Service Research Data Archive. https://doi.org/10.2737/RDS-2014-0030

Hudak, Andrew T.; Bright, Benjamin C. 2014(b). RxCADRE 2008, 2011, and 2012: Burn blocks. Fort Collins, CO: Forest Service Research Data Archive. https://doi.org/10.2737/RDS-2014-0031

Kochanski AK (2016) Modeling support for FASMEE experimental design using WRF-SFIRE-CHEM. *Joint Fire Sciences Project 16-4-05-3*.

Larkin NK, O'Neill SM, Solomon R, Raffuse S, Strand T, Sullivan DC, Ferguson SA (2010) The BlueSky Smoke Modeling Framework. *International Journal of Wildland Fire* **18**, 906-920.

Lavdas, LG (1996). Program VSMOKE—User's Manual. *General Technical Report SRS-6*. Asheville, NC: USDA Forest Service, Southern Research Station.

Linn RR 1997 A Transport Model for Prediction of Wildfire Behavior. *Los Alamos National Laboratory Science Report.* Los Alamos, NM, Los Alamos National Laboratory LA-13334-T.

Linn RR., Cunningham P 2005 Numerical simulations of grass fires using a coupled atmosphere-fire model: basic fire behavior and dependence on wind speed, *Journal of Geophysical Research-Part D-Atmospheres* **110** (D13).

Linn RR, Winterkamp K, Colman J, Edminster C 2005 Modeling interactions between fire and atmosphere in discrete element fuel beds. *International Journal of Wildland Fire* **14**(1): 37-48

Mandel J, Beezley JD, Kochanski AK (2011) Coupled atmosphere-wildland fire modeling with WRF 3.3 and SFIRE 2011. *Geoscientific Model Development* **4**, 591–610.

Mandel J, Amram S, Beezley JD, Kelman G, Kochanski AK, Kondratenko VY, Lynn BH, Regev B, Vejmelka M (2014) Recent advances and applications of WRF-SFIRE. *Natural Hazards and Earth System Science* **14**, 2829–2845.

McGrattan KB, Baum HR, Walton WD, Trelles J (1997) Smoke plume trajectory from in situ burning of crude oil in Alaska – field experiments and modelling of complex terrain *NISTIR 5958*, National Institute of Standards and Technology.

McNamara D, McNamara D, McNamara G (2016) Integrating Geographic Information Science (GISci) with the Study of Wildland-Urban Interface (WUI) and Wildland Fires: Modeling, Remote Sensing and Data Collection. National Institute of Standards and Technology Fire Research Grant Final Report. Accessed 5/1/17. https://gmsllc.box.com/s/vsyd93oua5mhc78di8qz75s5eudn19ok

McNamara D (2017) Fire and smoke modeling evaluation experiment (FASMEE) initial integrated data management plan. *Final report submitted to FASMEE leadership.* *https://gmsllc.box.com/s/x87pdchg4usmt0s08dm4vgtlf22j0wkz*

Mell WE, Jenkins MA, Gould J, Cheney P 2007 A Physics-Based Model for Grassland Fires, *Intl. J. Wildland Fire,* **16**: 1-27.

Mell WE, Maranghides A, McDermott R, Manzello SL 2009 Numerical simulation and experiments of burning Douglas firs trees, *Combustion & Flame*, **156**: 2023-2041

McNamara D (2015a) Integrating WUI fire models with GIS, Camp Swift, Texas, prescribed burn geospatial data integration, http://www.gmsgis.com/camp-swift-burns.html

McNamara D (2015b) Integrating and analyzing prescribed burn data with ArcGIS, *ESRI User Conference*, San Diego Convention Center, July 20-24 2015

Mueller EV, Skowronski N, Clark K, Gallagher M, Kremens R, Thomas JC, Housssami ME, Filkov A, Hadden RM, Mell W, Simeoni (2017) A Utilization of remote sensing techniques for the quantification of fire behavior in two pine stands, *Fire Safety Journal*, inpress

Paugam R, Wooster MJ. Roberts G, 2013 Use of Handheld Thermal Imager Data for Airborne Mapping of Fire Radiative Power and Energy and Flame Front Rate of Spread, *Geoscience and Remote Sensing, IEEE Transactions*, **51**(6), pp.3385-3399

O'Brien JJ, Loudermilk EL, Hornby B, Huday AT, Bright BC, Dickinson MB, Hiers JK, Teske C, Ottmar RD (2016) High-resolution infrared thermography for capturing wildland fire behavior – RxCADRE 2012, *International J. Widland Fire*, **25**: 62-75.

Ottmar RD, Hiers JK, Butler BW, Clements CB, Dickinson MB, Huday AT, O'Brien JJ, Potter BE, Rowell EM, Strand TM, Zajkowski (2016) Measurements, datasets and preliminary results from the RxCADRE project – 2008, 2011 and 2012, *International J. Wildland Fire* **25**: 1-9

Peterson DL and Hardy CC (2016) The RxCADRE study: a new approach to interdisciplinary fire research. *International J. Wildland Fire* **25**, i.

Rowell R, Apland E, Seielstad C 2013 Ground LIDAR Fuel Measurements of the Prescribed Fire Combustion and Atmospheric Dynamics Research Experiment. *IAWF 4th Fire Behavior and Fuels Conference.* Raleigh, North Carolina, February 18-22, 2013.

Rowell, Eric M.; Seielstad, Carl A.; Ottmar, Roger D. 2016. Development and validation of fuel height models for terrestrial lidar - RxCADRE 2012. International Journal of Wildland Fire. 25: 38-47.

Scott JH and Burgan RE (2005) Standard fire behavior fuel models: A comprehensive set for use with Rothermel's surface fire spread model, *RMRS General Technical Report RMRS-GTR-153*

Stocks BJ, Alexander ME, Lanoville RA (2004) Overview of the international crown fire modelling experiment (ICFME), *Canadian J. Forest Research* **34**: 1543-1547.

USDA Data Archive (2017) for RxCADRE experimental data. https://www.fs.usda.gov/rds/archive/Catalog?freesearch=RxCadre&pageIndex=2

Vodacek A, Kremens RL, Fordham AJ, Vangorden SC, Luisi D, Schott JR, Latham DJ (2002) Remote optical detection of biomass burning using a potassium emission signature, *International Journal of Remote Sensing*, **23**(13), 2721 - 2726.

Wooster MJ, Roberts GL, Perry W, Kaufman YJ 2005 Retrieval of biomass combustion rates and totals from fire radiative power observations: FRP derivation and calibration relationships between biomass consumption and fire radiative energy release*, J. Geophys. Res*., **110**, D24311, doi:10.1029/2005JD006318.

Zhukov B, Lorenz E, Oertel D, Wooster M, Roberts G 2006 Spaceborne detection and characterization of fires during the bi-spectral infrared detection (BIRD) experimental small satellite mission (2001–2004), *Remote Sens. Environ*., **100**, 29–51, doi:10.1016/j.rse.2005.09.019, 2006. 9830, 9831, 9860, 9863, 9890

Appendix A: Contact Information for Key Project Personnel

William Mell. Pacific Wildland Fire Sciences Laboratory, Rocky Mountain Research Station, 400 N. 34th St., Suite 201, Seattle, WA 98103. Email:
wemell@fs.fed.us
(206)430-2072

Co-Principal Investigators
Rod Linn, Earth and Environmental Sciences, Los Alamos National Laboratory, Los Alamos, NM
rrl@lanl.gov
(505)665-6254

Project Scientists

Eunmoo Koo, Earth and Environmental Sciences, Los Alamos National Laboratory, Los Alamos, NM
koo_e@lanl.gov
(505) 606-2180

Ronan Paugam, Visiting Scientist, University of Washington, School of Environmental and Forest Sciences, Seattle, WA
ronan.paugam@gmail.com

Appendix B: List of Completed and Planned Publications and Science Delivery Products

Conference Proceedings

Yongqiang L, Kochanski A, Baker K, Mell W, Linn R, Paugam R, Mandel J, Fournier A, Jenkins MA, Goodrick S, Achtemeier G, Hudak A, Dickinson M, Potter B, Clements C, Urbanski S, Ottmar R, Larkin N, Brown T, French N, Prichard S, Watts A, McNamara D (2016) Fire and Smoke Model Evaluation Experiment (FASMEE): Modeling Gaps and Data Needs, *Proceedings for the 2nd International Smoke Symposium* November 14-17, 2016, Long Beach, California, USA Published by the International Association of Wildland Fire, Missoula, Montana, USA

Conference Abstracts

Paugam R, J.-P. Gastellu-Etchegorry, W. Mell, J. Johnston, J.-B. Filippi (2017). Prescribed Burn, Helicopterborne Infrared Imagery, and 3D Plume Model for Synthetic FRP Product Simulation. Earth Observation Summit 2017.

Posters

Paugam R, J.-P. Gastellu-Etchegorry, W. Mell, J. Johnston, J.-B. Filippi (2016). Modelling Middle Infrared Thermal Imagery from Observed or Simulated Active Fire. AGU Fall Meeting.